GRI-8[illegible]/0193

NATURAL GAS I.C. ENGINE HEAT PUMP STUDY

FINAL REPORT

April 1983

Gas Research Institute
8600 West Bryn Mawr Avenue
Chicago, Illinois 60631

NATURAL GAS I. C. ENGINE HEAT PUMP STUDY

FINAL REPORT
(June 1981 - September 1982)

Prepared by
Sam V. Shelton, Ph.D.

School of Mechanical Engineering
Georgia Institute of Technology
Atlanta, Georgia 30332
Project No. E25-650

for
GAS RESEARCH INSTITUTE
Contract No. 5081-341-0503

GRI Project Manager
Les Wright
Gas Fired Heat Pumps

April 1983

GRI DISCLAIMER

0272-101

REPORT DOCUMENTATION PAGE	1. REPORT NO. GRI-81/0193 Final Report	2.	3. Recipient's Accession No.

4. Title and Subtitle
Natural Gas I.C. Engine Heat Pump Study

5. Report Date
April 1983

6.

7. Author(s)
Sam V. Shelton

8. Performing Organization Rept. No.
E25-650

9. Performing Organization Name and Address
Georgia Institute of Technology
School of Mechanical Engineering
Atlanta, Georgia 30332

10. Project/Task/Work Unit No.
GRI-81/0193

11. Contract(C) or Grant(G) No.
(C) 5081-341-0503
(G)

12. Sponsoring Organization Name and Address
gri - Gas Research Institute
8600 West Bryn Mawr Avenue
Chicago, Illinois 60631

13. Type of Report & Period Covered
Final Report
6/81-9/82

14.

15. Supplementary Notes
To experimentally assess the technical performance of a natural gas I.C. engine heat pump using commercially available technology.

16. Abstract (Limit: 200 words)

The I.C. engine heat pump is one gas heat pump technology which uses existing component technology; it therefore offers the possibility of early development of a commercially viable gas heat pump. In order to assess the development barriers, this project carried out field tests on an I.C. engine heat pump providing heating and cooling to a residence over two heating and two cooling seasons. Experimental results showed steady state and seasonal heating coefficients of performance (COP) of 1.4 to 1.5 with cooling COP's 0.5 to 0.6. These efficiencies were in spite of the low 16% efficiency of the 1600 cc four cylinder industrial engine due to being loaded only to about 25%.

Using experimental engine/compressor data in conjunction with an air-to-air heat pump system configuration model, seasonal heating COP's of 1.33, 1.45, and 1.53 were predicted for Chicago, Atlanta, and Orlando respectively. Cooling COP's were 0.73 in all three cities. Higher engine loading would improve all COP's. No maintenance was required for the 2400 hours of operation during two heating and two cooling seasons. Noise in the equipment room was 63 dB with 61 dB measured outside next to the exhaust outlet.

17. Document Analysis a. Descriptors

b. Identifiers/Open-Ended Terms

c. COSATI Field/Group

18. Availability Statement	19. Security Class (This Report)	21. No. of Pages
	20. Security Class (This Page)	22. Price

(See ANSI-Z39.18) — See *Instructions on Reverse* — OPTIONAL FORM 272 (4-77) (Formerly NTIS-35) Department of Commerce

Title	Natural Gas I.C. Engine Heat Pump Study
Contractor	Georgia Institute of Technology
Principal Investigator	S. V. Shelton, Ph.D.
Report Period	May 31 - October 1982 Final Report
Objective	To experimentally assess the technical performance of a natural gas I.C. engine heat pump using commercially available technology.
Technical Perspective	Space heating and cooling constitutes the major use of natural gas in the U.S. Increasing the efficiency of this process would, therefore, provide a dramatic impact on the industry. The I.C. engine heat pump is one gas heat pump technology which uses existing component technology; it therefore offers the possibility of early development of a commercially viable gas heat pump. In order to assess the development barriers, this project carried out field tests on an I.C. engine heat pump providing heating and cooling to a residence over two heating and two cooling seasons performance of the system.
Results	Experimental data from a gas I.C. engine water-to-water heat pump showed steady state and seasonal heating coefficients of performance (COP) of 1.4 to 1.5 with cooling COP's 0.5 to 0.6 These efficiencies were in spite of the low 16% efficiency of the 1600 cc four cylinder industrial engine which was due to being loaded only to about 25% of full load. Using experimental engine/compressor data in conjunction with an air-to-air heat pump system configuration model, seasonal heating COP's of 1.33, 1.45 and 1.53 were predicted for Chicago, Atlanta and Orlando respectively. Cooling COP's were 0.73 in all three cities. Higher engine loading would improve all COP's. No maintenance was required for the 2400 hours of operation during two heating and two cooling

seasons. Oil analysis showed the oil was fully servicable. The only reliability problems encountered were a few failures to start during a fixed five second starter engagement period. Noise in the equipment room was 63 dB with 61 dB measured outside next to the exhaust outlet.

The project has shown that automotive derivative gas industrial engines operating at low speed have the necessary efficiency, noise, maintenance, and short term reliability to serve as the prime mover for an I.C. engine heat pump. It is recommended that available small I.C. engines suitable for I.C. engine heat pumps be surveyed and that selected models be tested for long life characteristics. Also, it is recommended that an air-to-air system be field tested to verify performance and to study outside coil defrost control strategies.

Technical Approach

A West German manufactured water-to-water packaged gas heat pump was installed in an Atlanta residence and supplied all space heating and cooling over two heating and two cooling seasons. Well water was used as a heat sink and source and was disposed afterward into a creek. An inside water circulating loop carried either hot or chilled water produced by the heat pump through a water coil in the air handler. The hot water loop passed through the condenser, exhaust gas heat exhanger, and engine cooling jacket. The system was fully instrumented for both long term and transient data acquisition. Total accumulated heating and cooling energies were measured along with accumulated gas flow over entire seasons to calculate seasonal performance factors (seasonal COP's). Steady state and transient performance was measured by a microcomputer data acquisition system with a one minute time resolution. Performance of the engine/compressor subcomponent was also measured as a function of condenser and evaporator temperature. A model was developed to use this engine/compressor data in conjunction with air condenser and evaporator coils. Optimization of the indoor vs. outdoor coil size was established. Also, performance with varying combined total air coil sizes was calculated for Chicago, Atlanta, and Orlando.

Project Implications

GRI plans to initiate another program on internal combustion engine driven heat pumps with appropriate manufacturers. The intent is to develop a heat pump that will have a low unit cost and near term market entry. During the first half of 1983, discussions have taken place between GRI and candidate engine manufacturers to determine their interest in teaming with a qualified space conditioning manufacturer to develop a gas engine heat pump. Proposals are being evaluated, and a program will be initiated by the end of 1983.

TABLE OF CONTENTS

LIST OF TABLES

LIST OF ILLUSTRATIONS

SECTION I

INTRODUCTION

Background

Thermal environmental control presently accounts for the greatest percentage of total energy use in the residential and commercial sectors of the U.S. In 1977, the energy required for the heating and cooling of residential and commercial establishments alone represented 21% of the U.S. total energy consumption and two-thirds of the U.S. total natural gas consumption. Increasing the efficiency for space heating and cooling would therefore amount to a significant reduction in the nation's total energy use. From the second law of thermodynamics, the maximum efficiency possible for space heating and cooling is that obtained by the ideal (reversible) heat-driven heat pump, an efficiency over 3 times that of ideal natural gas furnaces and boilers. In practice, this ideal efficiency can be approached but never attained.

One of the more promising practical natural gas heat pump systems that has emerged in recent years is the natural gas, internal combustion (IC) engine-driven heat pump. This system offers an attractive efficiency (performance) for space heating, as compared with other heating system such as the gas furnace, electric heat pump, and electric resistance heating. At the same time, it is capable of a space cooling performance comparable to that of the electric heat pump (i.e., electric air conditioner).

In the U.S., I.C. engines serving as stationary prime movers were displaced in the 1930's and 1940's by electric drives accompanying the rural electrification program. Therefore, small [less than 2000 cc] I.C. engine technology in this country has moved toward high speed, short term, high specific power output to serve automobile, portable drive, and emergency drive applications. Therefore, in this country, small I.C. engines are not viewed as being applicable to stationary, high running hours service.

In Europe, however, the use of small I.C. engines in stationary applications is still considered viable and a small market has been maintained. These are low speed, lightly (50%) loaded engines which are designed specifically for the stationary application, or are automobile engines modified for that service.

For this reason, when energy prices escalated in the mid-70's, Europe started looking seriously at the I.C. engine heat pump as a viable energy conservation concept.

In September 1978, a conference on "Drive for Heat Pumps" was held at the University of Essen, West Germany at which the investigation of electric motors vs. combustion motors for heat pumps was the primary topic. The forward of the conference proceedings states: "This issue of Drives for

Heat Pumps, as well as the conference in Essen, show that either means of drive has its justification and that there is ample room for both of them on the market." Eleven of the 17 papers presented were on I.C. engine drives for heat pumps. One paper was a survey of 14 I.C. engine heat pump systems installed and operating. Since then, several hundred operating units have been installed in the field and major corporations have started development projects.

In order to assess experimentally the potential problems and opportunities for I.C. engine driven heat pumps, a heating and cooling system for a single family residence was designed, built, and tested around the Florian Bauer GWW 35 natural gas driven heat pump package manufactured in West Germany. This heat pump package has evolved over the past four years so that many of the packaging, noise, vibration, and accessory problems have now been resolved. Purchasing this package allowed this project to focus on the system concept rather than its peripheral problems. The objective was to identify experimentally the noise, vibration, reliability, and maintenance problems of the I.C. engine gas heat pump concept and to quantify the field efficiency of this particular system. The project results will allow a more accurate assessment of the potential of the I.C. engine heat pump than has been previously possible.

Fundamental Thermodynamics

The heat pump is a device which operates in a thermodynamic cycle and requires energy input to pump heat from a low temperature reservoir (heat source) to a high temperature reservoir (heat sink). As a heating system, the heat pump extracts heat from the surroundings (such as outdoor air or ground water) and delivers it, along with the heat equivalent of the energy input, to a conditioned space. By extracting heat from the surroundings, the heat pump makes more energy available for heating than is required for input. This gives the heat pump its dramatic advantage over conventional, direct heating systems. As a cooling system, the heat pump removes heat from a conditioned space and rejects its, with the heat equivalent of the energy input, to the surroundings.

The first law efficiency of a thermodynamic system is defined as the ratio of energy sought to energy that costs. For heat pumps, this ratio is expressed as the coefficient of performance. The energy sought is either the heating effect or the cooling effect, and the energy that costs is the energy input. The coefficient of performance based on work energy input is given the notation COPW, while COPH is used to denote the performance based on heat energy input. Subscripts H and C are used to indicate whether the energy sought is heating or cooling.

When energy is supplied to the heat pump in the form of heat, the result is a heat-driven heat pump. An energy flow diagram for the heat-driven heat pump is presented in Figure 1. As a result of heat input Q_S, at temperature T_S. a quantity of heat Q_C is removed from a reservoir at temperature T_C, and a quantity of heat Q_H is rejected to a reservoir at temperature T_H. From a simple energy balance on this system:

$$Q_S = Q_H - Q_C \tag{1}$$

and the coefficients of performance for heating and cooling are:

$$COPH_H = \frac{Q_H}{Q_S} = \frac{Q_H}{Q_H - Q_C} \tag{2}$$

$$COPH_C = \frac{Q_C}{Q_S} = \frac{Q_C}{Q_H - Q_C} = 1 - COPH_H$$

The maximum performance theoretically possible would be that achieved by a reversible heat-driven heat pump. From the second law of thermodynamics, the Clausius inequality requires that:

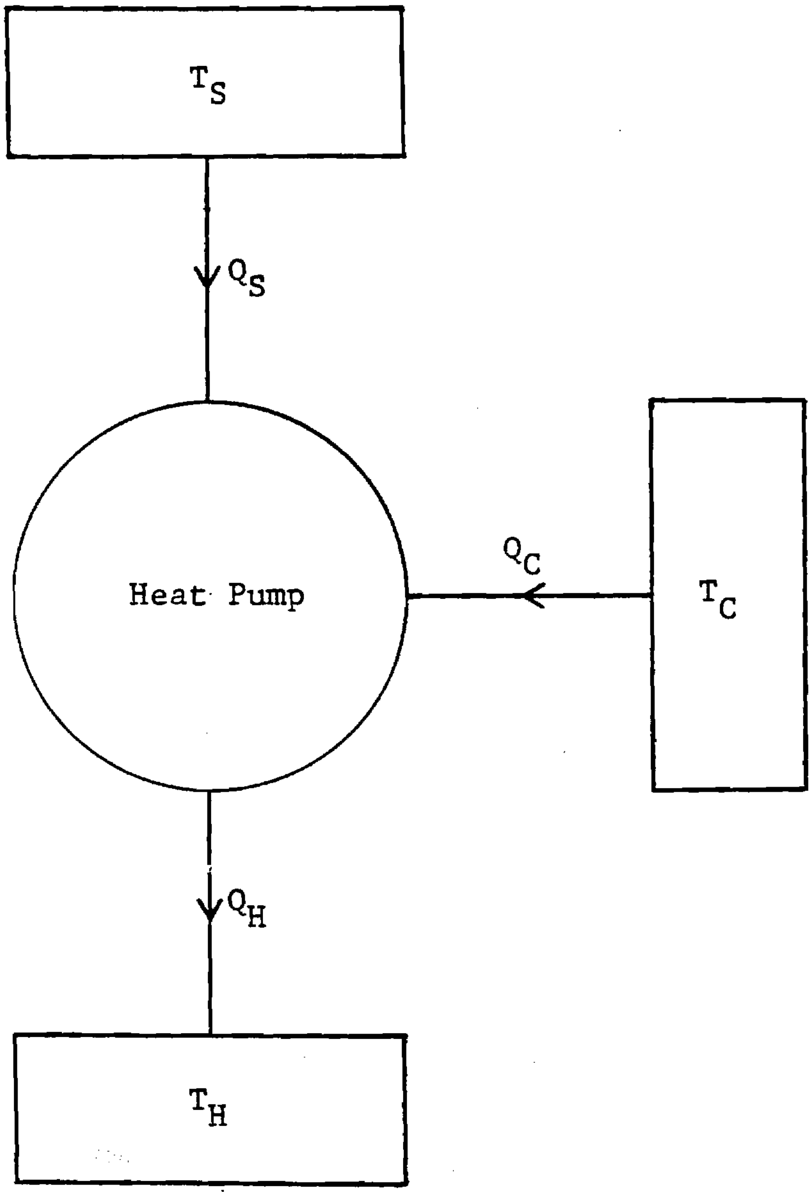

Figure 1. Energy Flow Diagram of a Heat-Driven Heat Pump

$$\oint \frac{\delta Q}{T} \leq 0 \tag{3}$$

where the equality holds for reversible processes. Then for the reversible heat-driven heat pump:

$$\oint \frac{\delta Q}{T} = \frac{\delta Q_S}{T_S} + \frac{\delta Q_C}{T_C} - \frac{\delta Q_H}{T_H} = 0 \tag{4}$$

or

$$\frac{Q_S}{T_S} + \frac{Q_C}{T_C} = \frac{Q_H}{T_H} \tag{5}$$

Combining equations (2) and (5), and simplifying, yields:

$$(COPH_H)_{rev.} = \left(\frac{1 - T_C/T_S}{1 - T_C/T_H}\right) \tag{6}$$

$$(COPH_C)_{rev.} = \left(\frac{T_C}{T_H}\right)\left(\frac{1 - T_C/T_S}{1 - T_C/T_H}\right)$$

$$= 1 - (COPH_H)_{rev.}$$

A system utilizing a Carnot cycle heat engine to drive a Carnot cycle heat pump would represent a reversible heat-driven heat pump. Such a system is shown in Figure 2. The heat engine operates between temperatures T_S and T_C to produce shaft work W_S. From an energy balance on the heat engine:

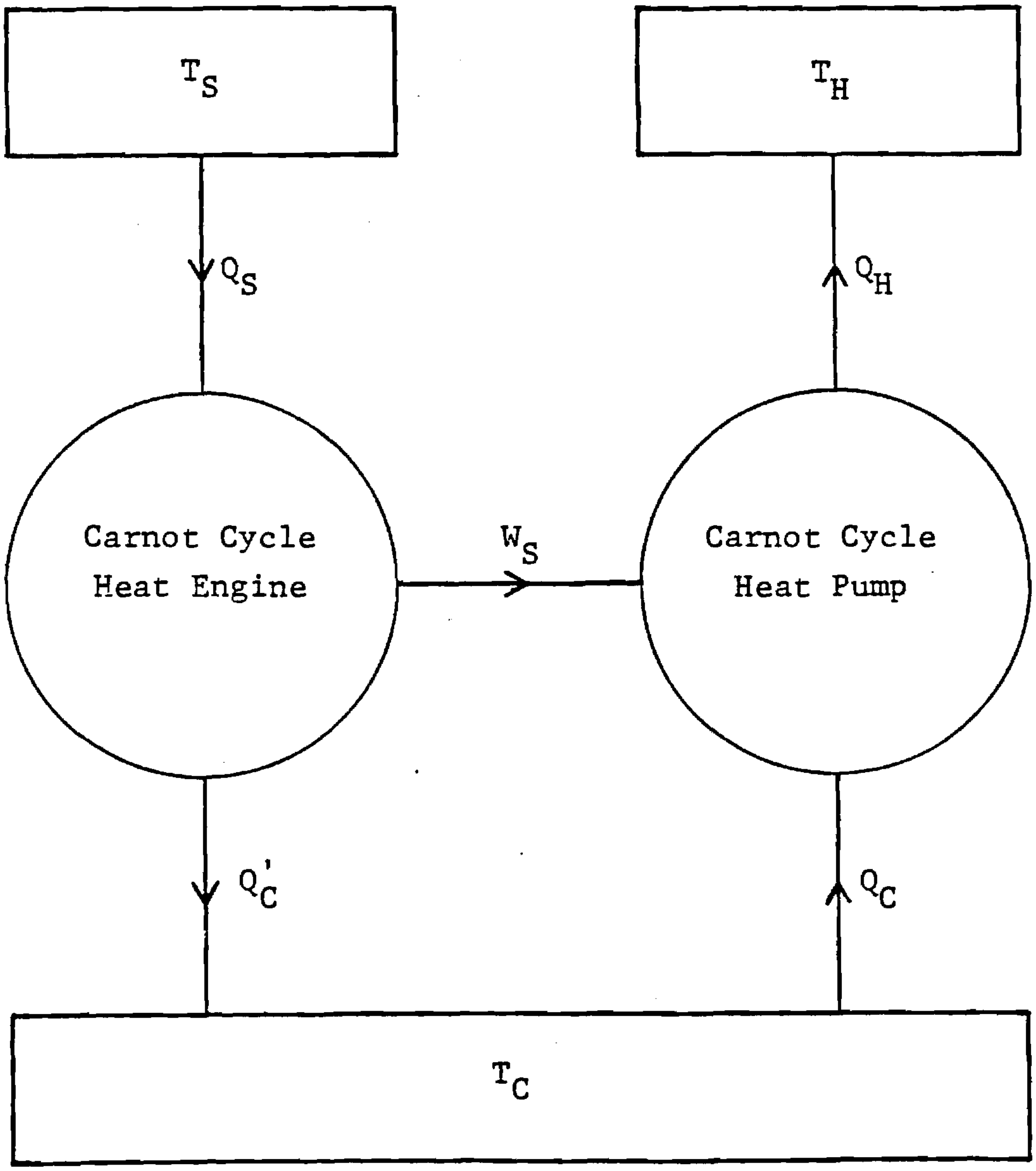

Figure 2. Energy Flow Diagram of an Ideal Heat Engine-Driven Heat Pump

$$W_S = Q_S - Q_C' \tag{7}$$

and the engine efficiency is:

$$\eta = \frac{W_S}{Q_S} = \frac{Q_S - Q_C'}{Q_S} \tag{8}$$

Since all processes of the Carnot cycle heat engine are reversible, equation (3) yields:

$$\frac{Q_S}{T_S} = \frac{Q_C'}{T_C} \tag{9}$$

Equation (8) then simplifies to:

$$\eta_{Carnot} = 1 - \frac{T_C}{T_S} \tag{10}$$

The heat pump receives work input, W_S, from the heat engine to remove heat, Q_C, from the reservoir at T_C and reject heat, Q_H, to the reservoir at T_H. From an energy balance on the heat pump:

$$W_S + Q_C = Q_H \tag{11}$$

and the coefficients of performance are:

$$COPW_H = \frac{Q_H}{W_S} = \frac{Q_H}{Q_H - Q_C} \tag{12}$$

$$\mathrm{COPW}_C = \frac{Q_C}{W_S} = \frac{Q_C}{Q_H - Q_C}$$

Since the Carnot cycle heat pump can be represented thermodynamically as a Carnot cycle heat engine operating in reverse, and all processes of the Carnot cycle heat engine are reversible, all processes of the Carnot cycle heat pump must also be reversible. Then equation (3) yields:

$$\frac{Q_H}{T_H} = \frac{Q_C}{T_C} \tag{13}$$

and equations (12) simplify to:

$$(\mathrm{COPW}_H)_{\mathrm{Carnot}} = \frac{1}{1 - T_C/T_H} \tag{14}$$

$$(\mathrm{COPW}_C)_{\mathrm{Carnot}} = \frac{T_C/T_H}{1 - T_C/T_H}$$

$$= 1 - (\mathrm{COPW}_H)_{\mathrm{Carnot}}$$

The products of equations (10) and (14) yield the coefficients of performance for the combined system (i.e., the ideal heat engine-driven heat pump):

$$(\mathrm{COPH}_H)_{\mathrm{Ideal}} = (n)_{\mathrm{Carnot}}(\mathrm{COPW}_H)_{\mathrm{Carnot}} \tag{15}$$

$$= \left(\frac{1 - T_C/T_S}{1 - T_C/T_H}\right)$$

$$(COPH_C)_{Ideal} = (\eta)_{Carnot}(COPW_C)_{Carnot}$$

$$= \left(\frac{T_C}{T_H}\right) \left(\frac{1 - T_C/T_S}{1 - T_C/T_H}\right) = 1 - (COPH_H)_{Ideal}$$

which are the same results obtained in equations (6).

Using typical temperatures for natural gas space heating/cooling, the ideal efficiencies for gas heat pumps may be calculated and compared with the ideal efficiencies of one for furnaces and boilers. For heating, typical values of T_C, T_S, and T_H are 20^oF, 1000^oF, and 140^oF resulting in a $COPH_H$ of 3.7. For typical space cooling values of 50^oF, 1000^oF, and 120^oF for T_C, T_S, and T_H respectively, $COPH_C$ is 5.4. This demonstrates the potential of the concept.

In practice, the Carnot cycle heat engine and Carnot cycle heat pump cannot be achieved because they require that all processes be reversible. Actual processes involve irreversibilities, such as frictional losses and heat transfer through finite temperature differences. An actual cycle can, at best, only approach the Carnot cycle efficiency or performance for a given application.

For heat pumps, the Carnot cycle performance is best approached by the actual vapor-compression cycle, which is shown schematically and on a temperature-entropy (T-S) diagram in Figure 3.

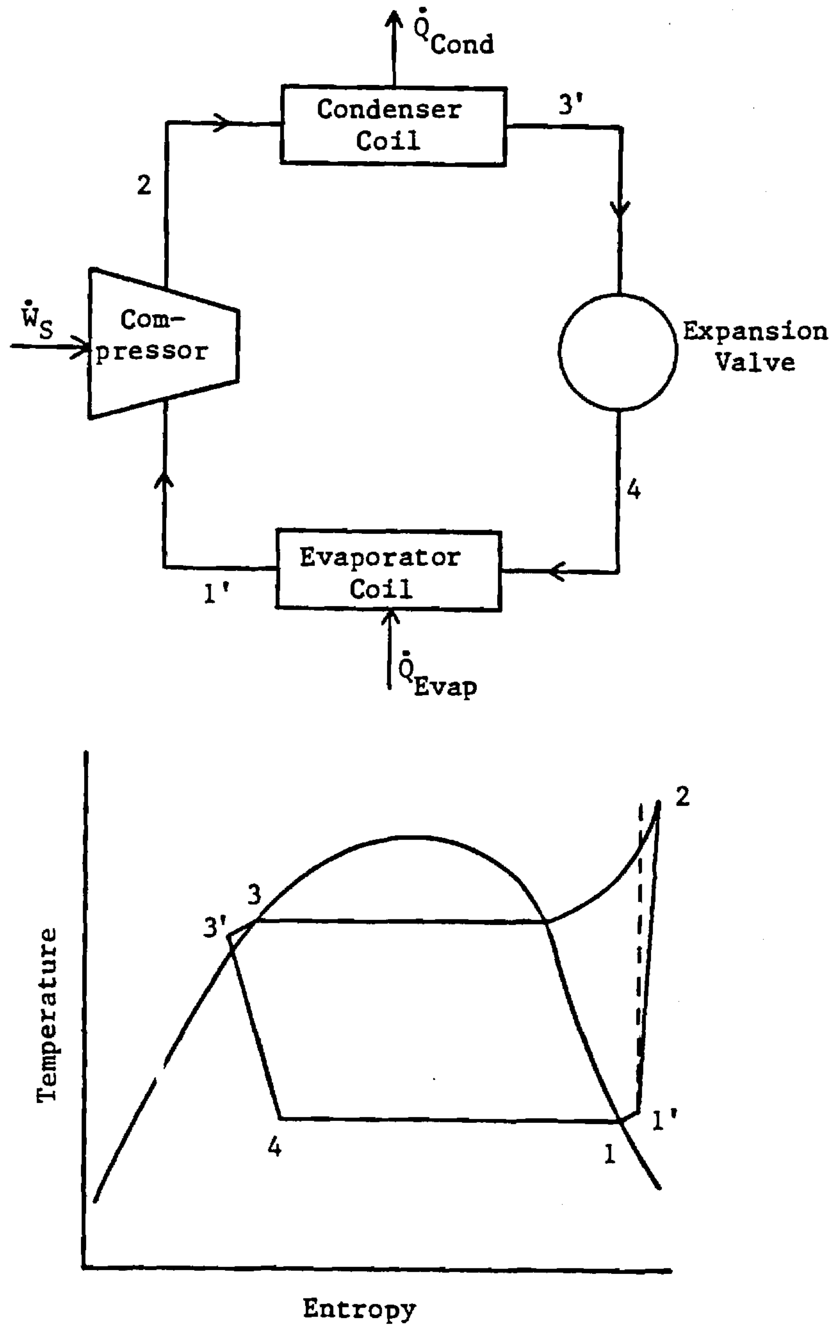

Figure 3. Schematic and T-S Diagram of Actual Vapor-Compression Cycle

For the vapor-compression cycle heat pump, work is input to the compressor at a rate $\dot{W}_S$, heat is removed from a low temperature reservoir by the evaporator coil at a rate $\dot{Q}_{Evap}$, and heat is rejected to a high temperature reservoir from the condenser at a rate $\dot{Q}_{Cond}$. The heating and cooling coefficients of performance are then:

$$COPW_H = \frac{\dot{Q}_{Cond}}{\dot{W}_S} \tag{16}$$

$$COPW_C = \frac{\dot{Q}_{Evap}}{\dot{W}_S}$$

The natural gas-fired IC engine provides one means for approaching the efficiency of the Carnot cycle heat engine. In an IC engine, the working fluid operates on an open cycle. Fuel is mixed with air, and the resulting gas mixture is ignited in one of the combustion chambers of a spark ignition engine. The product gas (or exhaust gas) is then released from the chamber and rejected to the surroundings. In the combustion process, the chemical energy of the fuel is converted to thermal energy. Some of the thermal energy is then converted to mechanical energy (shaft work) through the use of reciprocating pistons. The thermal energy that is not converted to shaft work is the engine rejected heat, a fraction of which is dissipated through the engine block. The remainder is carried away by the exhaust gas.

For the I.C. engine, the energy rate sought is the shaft work rate $\dot{W}_S$, and the energy rate that costs is the gas input rate $\dot{Q}_{Gas}$. The gas input rate is a product of the heating value of the fuel and the rate of fuel consumption. The heating value (Frequently termed "energy of combustion" or "heat of reaction") is a measure of heat transfer from a constant volume chamber during combustion at constant temperature. The first law efficiency of the I.C. engine is then:

$$\eta_{Eng} = \frac{\dot{W}_S}{\dot{Q}_{Gas}} \qquad (17)$$

It follows that the engine rejected heat rate is:

$$\dot{Q}_{Eng} = (1 - \eta_{Eng})\dot{Q}_{Gas} \qquad (18)$$

When the I.C. engine is utilized strictly for performing work, the engine rejected heat is not useful and is commonly released to the surroundings. On the other hand, when the I.C. engine is used to drive a heat pump for which heating is the energy sought, the engine rejected heat is useful if it can be recovered. Therefore, a major advantage of the I.C. engine-driven heat pump is its potential for utilizing heat that is normally wasted.

The work of an actual heat-driven heat pump results from the use of a natural gas-fired I.C. engine to drive the compressor of a vapor-compression cycle heat pump. If a fraction, ε, of the engine rejected heat is recovered through some type of heat exchange process, then an additional rate of heat, $\dot{Q}_{Rec}$, is available for space heating. From equation (18):

$$\dot{Q}_{Rec} = \varepsilon\dot{Q}_{Eng} = \varepsilon(1 - \eta_{Eng})\dot{Q}_{Gas} \tag{19}$$

Then for the actual heat-driven heat pump, the coefficients of performance obtained from equations (16), (17), and (19) are:

$$COPH_H = \frac{\dot{Q}_{Cond}}{\dot{Q}_{Gas}} + \frac{\dot{Q}_{Rec}}{\dot{Q}_{Gas}} = \eta_{Eng}COPW_H + \varepsilon(1 - \eta_{Eng}) \tag{20}$$

$$COPH_C = \eta_{Eng}COPW_C = \frac{\dot{Q}_{Evap}}{\dot{Q}_{Gas}}$$

These are the coefficients of performance referred to throughout the remainder of this text.

Using off-the-shelf advanced technology, reasonable hardware values for an I.C. engine heat pump are:

$$\eta_{Eng} = 0.25$$

$$\varepsilon = 0.8$$

$$COPW_H = 4$$

$$COPW_C = 4.$$

These values show that the present available component hardware potential is 1.6 for $COPH_H$ and 1.0 for $COPH_C$. A diagram of the I.C. engine heat pump concept using this available component technology is shown in Figure 4.

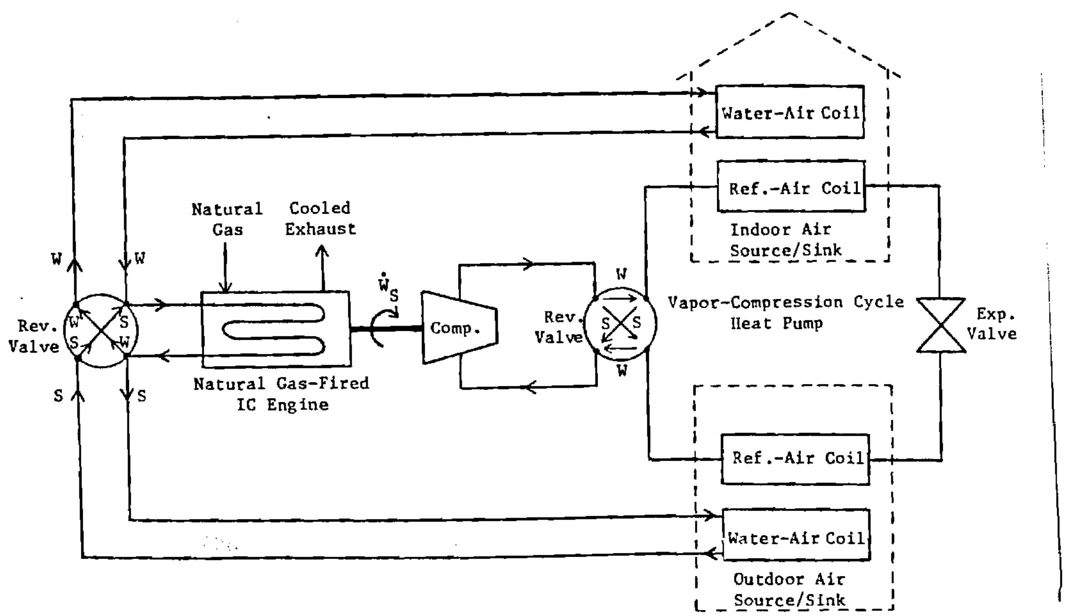

Figure 4. I.C. Engine Heat Pump Concept

SECTION II

I. C. ENGINE HEAT PUMP SYSTEM DESIGN

Description of Experimental System

The experimental system consists of a Florian Bauer GWW 35 natural gas driven heat pump package with an accessory exhaust gas/water heat exchanger for recovery of engine rejected heat, an integrated air/water heat exchanger with a central air handling system, and instrumentation.

The Florian Bauer GWW 35 heat pump package utilizes a 1600 cc four cylinder spark ignition engine built by the Ford Motor Company of Europe to drive a vapor compression cycle heat pump. This package, manufactured and marketed in West Germany, was designed to provide hot water for space heating via a radiator system, as is common practice in Europe. The manufacturer's specifications for this heat pump package appear in Table 1. It was also designed to use underground water rather than outdoor air as the external heat source/sink.

This water source system is not the development goal for gas heat pumps, because applications using underground water along with a water disposal sink (injection or stream) are limited. However, the prime subcomponent under question in I.C. engine heat pumps is the engine/compressor. This system allows testing of this major subcomponent without the added development effort to design and construct the outdoor coil,

Table 1. Florian Bauer GWW 35 Heat Pump Specifications

Maximum Heating Output @ 1800 rpm:	129,700 Btu/hr
Fuel Consumption Rate:	84.9 ft^3/hr
$COPH_H$ at Maximum Output:	1.49
Required Water Flowrate @ 50°F Water Temperature:	15.4 gallons per minute
Weight:	1,430 lb.
Length:	53 inches
Width:	34 inches
Height:	52 inches

refrigeration reversing valve, and defrost controls. It was believed that these outdoor air coil problems should be decoupled from the engine/compressor testing and focused on after the engine/compressor was proven quiet and reliable with satisfactory maintenance.

This water-to-water heat pump was integrated with an air duct system for producing heated and cooled air for space conditioning. A water-to-water heat pump has both an advantage and disadvantage with respect to an air-to-air system. In heating, the well water evaporator is advantageous over an outside air evaporator, but the hot water producing condenser will be at a disadvantage compared to an air condenser placed directly in the air handler. In the cooling mode, the well water cooled condenser will be advantageous over an outside air condenser, but the chilled water evaporator will be at a disadvantage compared to an air evaporator placed directly in the air handler. In short, a water-to-water system has the advantage of a well water "outside" coil but the disadvantage of having two inside heat exchangers in series, i.e. refrigerate-to-water and water-to-air rather than a single refrigerate-to-air.

An air-water heat exchanger and central air handling system was integrated with the Florian Bauer heat pump to provide heated and cooled air for space conditioning. Heat is exchanged between a circulating water loop and house air in an air handler with an ARKLA 5-ton vertical chill water coil, model number 60-136. The coil has a UA value of approximately 4500 Btu/hr-^{O}F. Indoor air is circulated through the coil by a blower in the air handler with 1/2 hp at a flow rated at 2000 cfm. Hot or cold water is circulated through the coil at a rated 10 gpm by one of two March Model 830, 1/5 HP pumps. An underground well behind the residence supplies water at approximately 60^{O}F year-round as the external heat source/sink for this system. The well water is pumped at a rated 6 gpm through one of the heat pump heat exchanger coils by a self-priming Teel 1-1/2 inch, 1/2 HP pump.

The well was drilled with a small portable drilling rig to a total depth of twenty-nine feet. A well screen and two-inch PVC casing were inserted and cemented in place. A series of pumping tests were conducted, demonstrating that the well could supply ground water at a rate approximating ten gallons per minute for a sustained period of time. After the water has been utilized as a heat sink/source, it is disposed of in Burnt Creek, which flows behind the residence. This plan of disposal has been approved by the Georgia Department of Natural Resources. An alternate plan of disposal that implemented a recharge well was discarded due to the convenience the creek offered and to its close proximity to the installation.

The Florian Bauer GWW 35 heat pump package was designed to provide heat recovery from the engine jacket and the exhaust manifold. As an accessory to this package, an external exhaust gas/water heat exchanger is utilized to recover additional engine exhaust rejected heat.

The experimental system was designed to provide space heating and cooling and domestic hot water. In winter, the system can provide space heating ("Mode 1") or it can heat water for domestic use ("Mode 2"). In the summer, the experimental system can provide simultaneous space cooling and domestic water heating ("Mode 3") or it can provide only space cooling when the domestic hot water storage tank is fully heated ("Mode 4").

A configuration of the experimental system is shown in Figure 5. The system employs seven manually operated valves, two automatic valves, two circulation pumps, and a well pump. The manual valves are opened or closed only when it is desired to change between the winter and summer modes. Essentially, the manual valves perform the same function as a heat pump refrigerant reversing valve. The automatic valves and pumps are thermostatically controlled in order to change operating modes in a given season of the year (i.e., between Modes 1 and 2, or between Modes 3 and 4). Table 2 provides a summary of valve positions and pump operation for each of the four modes of operation.

System Control

The system is controlled in an on/off manner. The four modes (2 winter and 2 summer) were chosen by a Smart-Stat solid state house thermostat and the domestic hot water

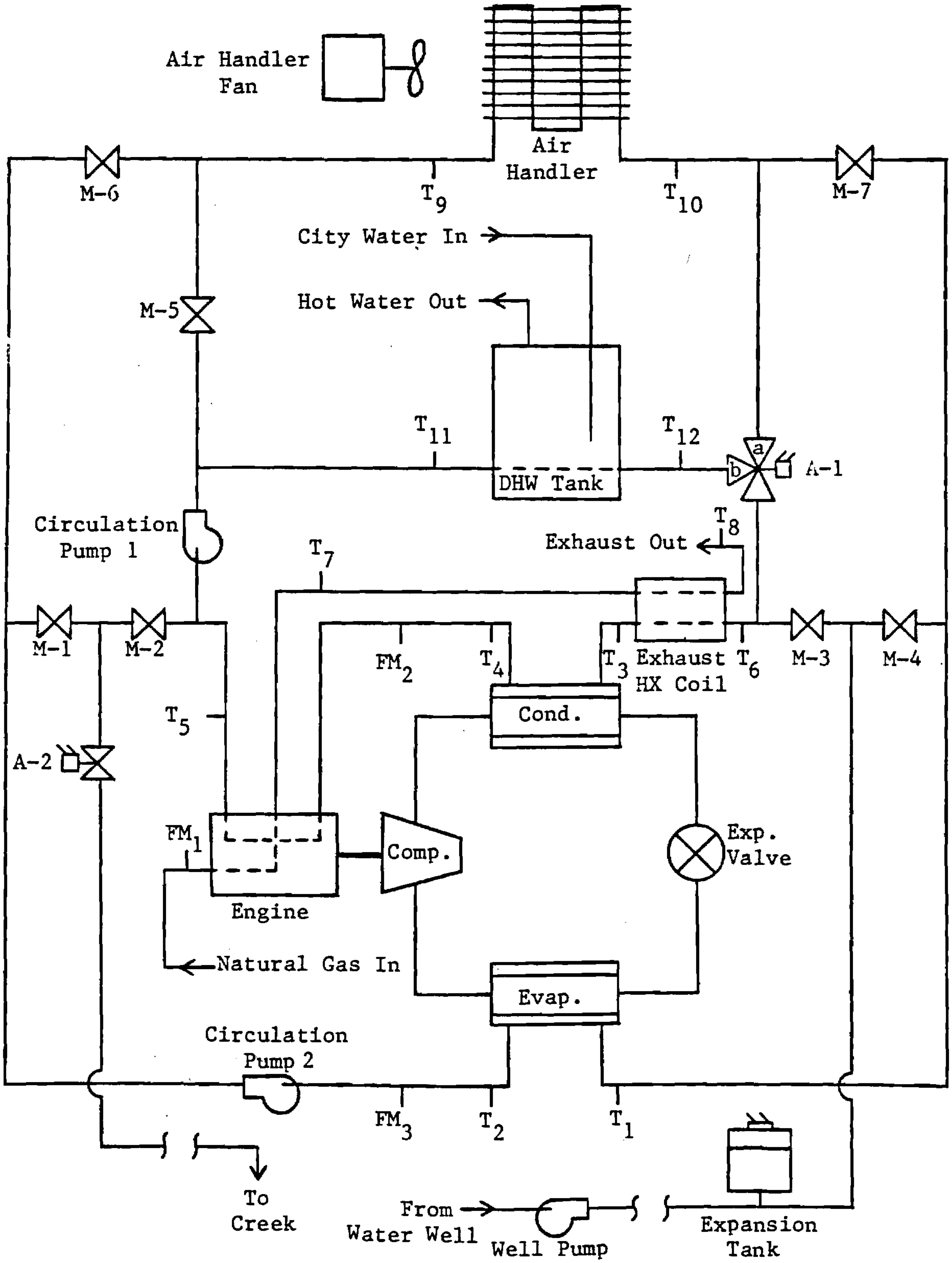

Figure 5. Experimental System Schematic

Table 2. Experimental System Valve Positions and Pump Operation

Winter (Space Heating) Mode 1 Valve A-1 in position "a" Valve A-2 OPEN Pump P-1 ON Pump P-2 OFF Well Pump ON Mode 2 Valve A-1 in position "b" Valve A-2 OPEN Pump P-1 ON Pump P-2 OFF Well Pump ON	MANUAL VALVES Valve M-1 OPEN Valve M-2 CLOSED Valve M-3 CLOSED Valve M-4 OPEN Valve M-5 OPEN Valve M-6 CLOSED Valve M-7 CLOSED
Summer (Space Cooling) Mode 3 Valve A-1 in position "b" Valve A-2 CLOSED Pump P-1 ON Pump P-2 ON Well Pump OFF Mode 4 Valve A-1 in position "a" Valve A-2 OPEN Pump P-1 OFF Pump P-2 ON Well Pump ON	MANUAL VALVES Valve M-1 CLOSED Valve M-2 OPEN Valve M-3 OPEN Valve M-4 CLOSED Valve M-5 CLOSED Valve M-6 OPEN Valve M-7 OPEN

thermostat. The winter space temperature control points are 69^{o}F-on/72^{o}F-off, with summer conditions set at 77^{o}F-on/74^{o}F-off. The thermostat time clock provided winter set back to 55^{o}F from 11:00 PM to about 6:00 AM. The actual morning reset time was determined by the Smart-Stat's optimal warmup strategy which reset the thermostat as necessary to reach 72^{o}F by 6:30 AM. The domestic hot water temperature setting varied but was typically 110^{o}-on/130^{o}F-off.

The thermostats provided 24 volt control signals to a group of relays which controlled the circulating pumps, air handler fan, and engine/heat pump. Also, 3 two position (winter/summer) toggle switches were incorporated with the relays to choose the space heating modes vs. the space cooling modes.

The priority of the two possible modes in each season was set as follows:

(1) Winter: Space heating was taken as priority over domestic water heating (DWH). If the heat pump was in the DWH mode when space heating was called for, the relays would immediately switch the system to the space heating mode.

(2) Summer: Two modes were possible: space cooling with simultaneous DWH, and space cooling with rejected heat to the outside. DWH without simultaneous space cooling was not possible. When space cooling was called for, the system

simultaneously heated water if the tank temperature was below 130^{o}F. If the tank was above 130^{o}F, the system would reject its heat outside. The domestic hot water thermostat would bring on DWH when the tank dropped below 110^{o}F. In this case, it would always simultaneously cool the house regardless of the room thermostat condition.

Providing space cooling in the summer when DWH was required, regardless of the space temperature, did not overcool the house except during some cool summer mornings when 4 showers would be taken during a 30 minute period. This condition however, provided stored cooling so that thermostat demand for space cooling was delayed until later in the day.

The relay controls are shown in Figure 6. This is the detailed relay circuit controlling the circulating pumps, air handler, and engine/heat pump. The engine/heat pump was activated by closure of CR-1, 2, or 3. At this point, starting of the engine/heat pump was carried out by separate controls in the engine/heat pump package. The starter was engaged for a period of 5 seconds, and the compressor bypass solenoid valve (to prevent starting against a compressor load) was opened for a period of 10 seconds. If the engine failed to sense oil pressure within 10 seconds, the engine/heat pump shut down on default, requiring a manual reset to reinitiate the starting cycle. These engine/heat pump starting controls were provided as part of the package by Florian Bauer.

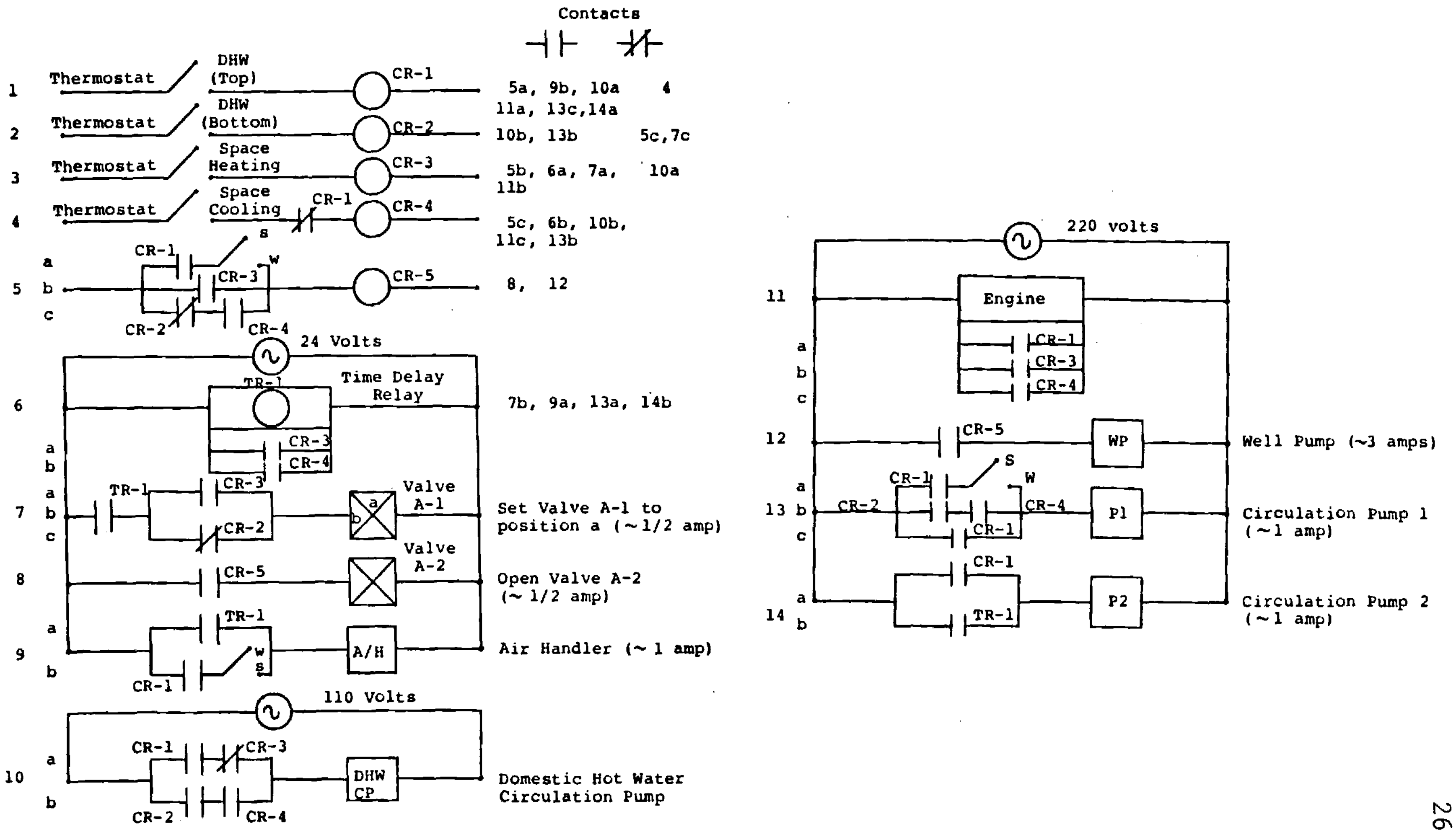

Figure 6: Heat Pump System Controls

SECTION III

INSTRUMENTATION

Long Term Monitoring

The monitoring of the heat pump over long time periods required an accumulating instrumentation system to accumulate 1) gas usage, 2) heat output, 3) cooling output, and 4) run hours.

The natural gas input was measured by installing a meter on the gas line leading to the engine. This meter is of the same type used by a gas utility company to measure domestic consumption for billing purposes. An hour meter was installed on the heat pump to measure the cumulative run time. The accumulated gas consumption could then be read from the meter and the average rate of gas consumption could be calculated by dividing the net gas consumption by the measured run time.

Energy supplied by the hot and chilled water loops was measured through the use of a pair of RHO-SIGMA model RS-805 Btu meters; they employ a flowmeter and a pair of temperature sensors placed in the supply and return of the respective hot and chilled water circuits. The Btu meters display the cumulative number of gallons of water that have flowed and the cumulative number of Btu's of heat transferred in the heated and chilled water circuits. The heating and cooling rates can be calculated by dividing the net number of Btu's of heat transferred by the run time.

The BTU meter thermisters have a manufacturer's stated precision of $\pm$ 0.4^{o}F with a nonlinearity which "does not have a measurable effect on the Btu-meter." The signals from the thermisters enter the RS-805 two bridge resistors which are matched to an accuracy of $\pm$ 0.04%.

The arithmetic circuitry directly measures the temperature difference between the two sensors rather than the absolute temperature of the sensors. This direct measurement minimizes signal processing which can introduce error. The temperature difference is converted to a digital signal through use of a digitally generated voltage staircase specifically shaped to eliminate the remaining non-linear influences of the thermisters. The 255 steps in the staircase determine the 1^{o}F resolution of the temperature differential measurement. One step is generated for each 1^{o}F.

The flow meters are a Kent model number C-700-FE (plastic) on the cold water circuit producing 4 pulses per gallons, and a RS-807B (brass) on the hot water circuit producing 200 pulses per gallon. The maximum stated error of the flow meters above 0.5 gpm is $\pm$ 1%. The pulses from the flowmeters trigger the voltage staircase which in turn triggers an oscillator in phase with the staircase. A positive temperature differential opens a gate which feeds the oscillator pulses into a counter. The number of pulses sent to the counter is directly proportional to Btus. When the counter accumulates the equivalent of 1,000

Btus, it increments a 6-digit counter and resets the circuitry. The overall stated accuracy for the Btu meters with a $10^{o}F$ water ΔT, which was typical, is $\pm$ 5%.

Computer Data Acquisition

In order to obtain more detailed data on the heat pump system's performance, a data acquisition system was designed and implemented to allow measurement of 12 temperatures, 2 water flow rates, natural gas flow rate, and all energy flow rates with a time resolution of 1 minute. The data system used an Apple II microcomputer with an ISAAC A/D interface made by Cyborg Corp.

Twelve thermocouple millivolt outputs were conditioned by 12 Analog Devices 252A amplifiers with internal reference. These 0 to 5 volt signals were fed into the ISAAC where they were digitized on a 0 to 4096 count scale and read by the computer on command. The location of the 12 thermocouples is shown in Figure 5.

Two counter channels in the ISAAC accumulate 0 to 5 volt pulses from the same two Kent water flow meters used by the Rho Sigma Btu meters previously described. These hot and cold loop water meters produce 200 pulses per gallon and 4 pulses per gallon, respectively. A third counter channel accumulates pulses from a DARCOM encoder fitted to the 1/4 cubic foot per resolution dial of the gas meter. This magnetic activated pulser produced five 0 to 5 volt pulses per revolution and was input to the ISAAC. These three counter channels were read each minute by the computer, which automatically zeroed the counters, giving flow rate per minute.

Additionally, two binary input ISAAC channels read the on/off status of control relays which determined when the system was on and which of the four operating modes the system was in.

The 12 bit digital thermocouple readings and 16 bit flow rate readings were read by the computer each minute after startup. The ISAAC's internal calender/clock supplied the day of week, date, hour, minute, and second for these readings. A complete system calibration was carried out on the thermocouple channels by placing all thermocouples, along with a mercury thermometer certified to a $\pm$ 0.1^{o}C accuracy, in a 50^{o}C ice bath and boiling water bath. A second order calibration curve was derived for each thermocouple channel to convert the counts to degrees C.

A basic language program was written for the Apple II which, upon heat pump startup, would log the time and date and read all data channels each minute. The energy flows were calculated as follows:

$$\dot{Q}_{Gas} = \dot{V}_{Gas}\ (1028\ \text{Btu/ft}^3)$$

$$\dot{Q}_{Cond} = (\dot{m}C_p)_{Cond}(T_4 - T_3)$$

$$\dot{Q}_{Evap} = (\dot{m}C_p)_{Evap}(T_1 - T_2)$$

The total rate of engine rejected heat recovered was determined by:

$$\dot{Q}_{Rec} = \underbrace{(\dot{m}C_P)_{Cond}(T_4 - T_5)}_{\begin{bmatrix}\text{Engine Jacket} \\ \text{+Exhaust Manifold}\end{bmatrix}} + \underbrace{(\dot{m}C_p)_{Cond}(T_6 - T_3)}_{\begin{bmatrix}\text{Exhaust Heat} \\ \text{Exchanger}\end{bmatrix}}$$

Minute by minute COP's were calculated by the program with:

$$COPH_C = \dot{Q}_{Evap}/\dot{Q}_{Gas}$$

$$COPH_H = (\dot{Q}_{Cond} + \dot{Q}_{Rec})/\dot{Q}_{Gas}$$

A complete schematic of the data acquisition system is shown in Figure 7. All data was converted to engineering units.

This temperature and flow rate data, with calculated energy flow rates and efficiencies, was then printed on the screen, paper printer, or floppy disk, as appropriate. An accumulating subroutine was used to yield accumulative run times, energy flow, and efficiencies in longer term tests.

INSTRUMENTATION SCHEMATIC

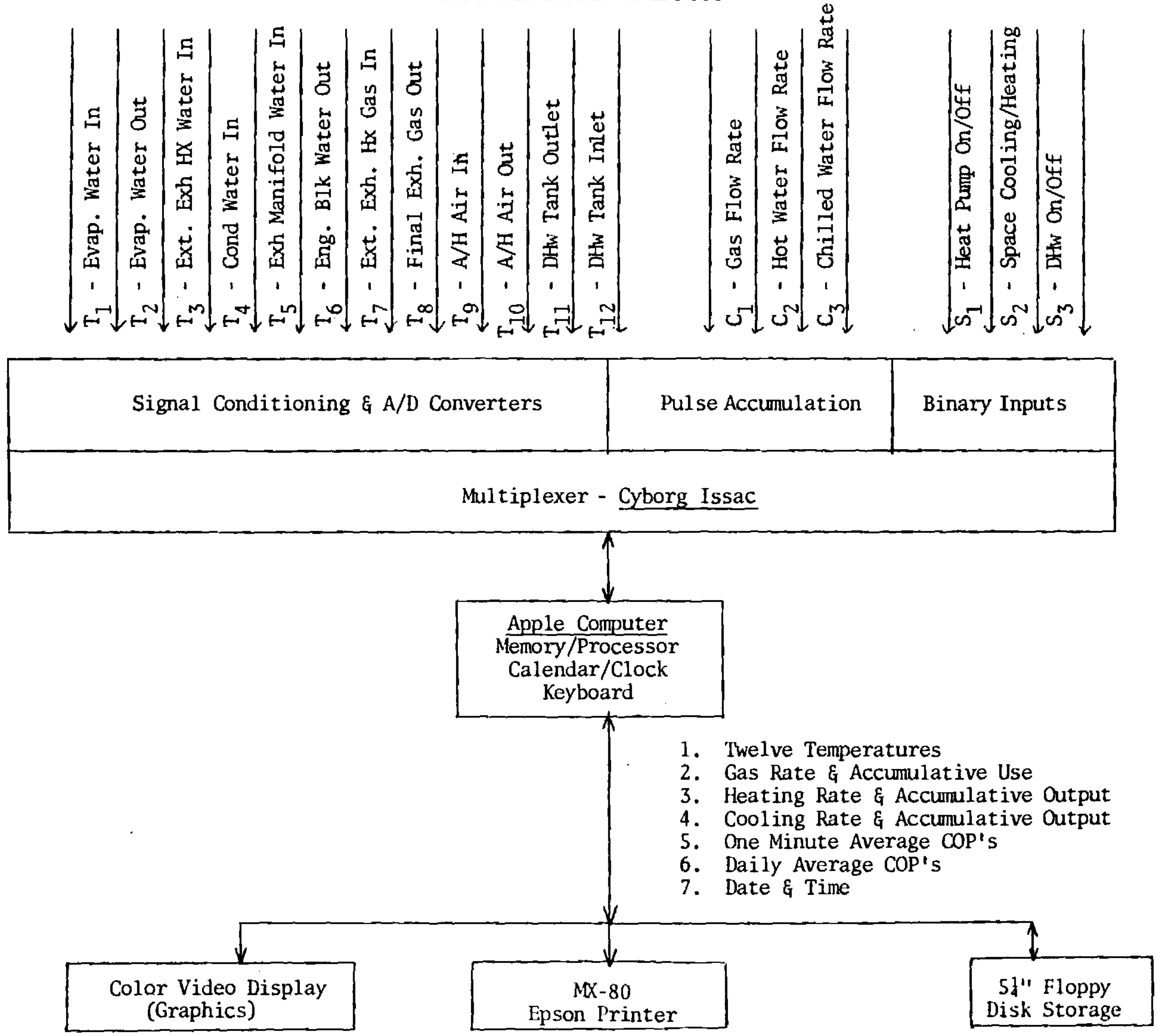

Figure 7: Computer Data Acquisition Schematic

SECTION IV

EXPERIMENTAL PERFORMANCE

Introduction

The Florian Bauer heat pump package was received from West Germany in December 1980. It was integrated into a residential heating/cooling system during early 1981, and since June 1981, has provided the space heating/cooling for the residence.

The residence is a 3200 square foot three story brick structure with glass composing 50% of the southeastern wall. This glazing has a ten foot overhang for summer shading. The structure was built in 1965. A five ton electric air conditioner was installed in 1965, with a 200,000 Btu/hr furnace installed in 1976. Hot water was supplied by a 40 gallon gas water heater installed in 1976. The house thermal "UA" value is about 680 Btu/hr-oF.

Analysis of data from 1978 to 1980 showed that natural gas consumption for space heating averaged 1000 therms annually with the furnace operating about 500 hours per year. An hour meter was installed on the electric air conditioner from 1979 to 1980 showing an average of 525 hours per year with 4200 kwhr electrical consumption annually.

Seasonal data was accumulated by the Btu and gas meters during the summer of 1981 and winter of 1981-82. In early

1982 the computer data acquisition system was installed, allowing more accurate data acquisition with one minute time resolution. During the summer of 1982, the Btu meters were checked against the computer data acquisition system. Both steady state and transient data were then taken to determine performance in detail.

Seasonal Performance

The system became operational on June 13, 1981 and the Btu meters became fully operational July 24, 1981. The system was closely monitored as it provided space cooling until October 13, 1981 when the heat pump cooling run time was 547 hrs. On almost a daily basis, the gas meter, hot and chilled water Btu meters, and heat pump hour meter were read and recorded. An abbreviated tabulation of this data is shown in Table 3. The engine speed was fixed at 1200 rpm.

In January 1982, new thermisters were installed on both Btu meters, since questions had arisen regarding the Btu meter accuracy. There was a slight (5%) reduction in the hot water Btu output after the new calibrated thermisters were installed. At the end of February 1982, a time delay relay was added to keep the air handler fan and air coil water circulating pump on for 6 minutes after the engine turned off. This "spindown" recovered additional heat from the engine. The system ran in the space heating mode until May 24, 1982, when it was then switched to cooling. On October 18, 1982, it was again switched to heating.

TABLE 3

Long Term Performance Raw Data

Date	Run (Hrs)	V_{Gas} (100 ft^3)	Q_{Heat} (1000 Btus)	Q_{Evap} (1000 Btus)
7/27/81	401	2,317	18,441	13,143
9/10/81	534	2,403	20.434	18,130
10/13/81	547	2,411	32,192	18,710
10/13/81	---------- Switched to Heating----------			
10/13/81	547	2,411	32,192	18,710
12/08/81	682	2,505	44,877	22,801
01/02/82	827	2,600	59,014	27,720
01/30/82	1,048	2,747	81,361	34,903
01/30/82	--------New Thermisters Installed-------			
02/28/82	1,188	2,836	93,721	39,524
02/28/82	--------Added A/H Fan and Pump Delay----			
03/31/82	1,288	2,897	102,600	42,792
05/0282	1,306	2,909	104,180	43,364
05/29/82	1,339	2,929	107,274	44,388
05/29/82	--------Switched to Cooling------------			
05/29/82	1,339	2,929	107,274	44,388
06/26/82	1,413	2,978	114,826	47,016
07/31/82	1,539	3,063	128,302	52,419
08/18/82	1,631	3,124	137,975	55,569
09/09/82	1,731	3,178	146,981	59,164
10/18/82	--------Switched to Heating------------			
10/18/82	1,731	3,206	151,926	Broken
04/19/83	2,402	3,646	218,705	------

All readings have been plotted against run hours and a least squares straight line was fitted to each season's segment. The results agree with merely taking the seasonal incremental accumulative numbers and dividing by the incremental seasonal run time. The following resulted:

Season	Run (Hrs)	$\dot{Q}_{Gas}$ (Btu/hr)	$\dot{Q}_{Heat}$ (Btu/hr)	$COPH_H$	$\dot{Q}_{Evap}$ (Btu/hr)	$COPH_C$
Summer 81*	146	66,000	94,000		38,100	0.58
Winter 81-2	792	67,100	94,800	1.41	32,400	
Summer 82	415	68,500	107,600		39,500	0.58
Winter 82-3	648	69,700	103,100	1.48		

*Partial Summer starting 7/24/81. Full summer hours - 547.

These results are summarized graphically on the heat pump system schematic in Figure 8 for heating and Figure 9 for cooling. In these figures, the values for the two heating seasons are averaged and the two cooling seasons were averaged to get overall heating and cooling performance. They represent Seasonal Performance Factor values.

FIGURE 8: SEASONAL SYSTEM HEATING PERFORMANCE

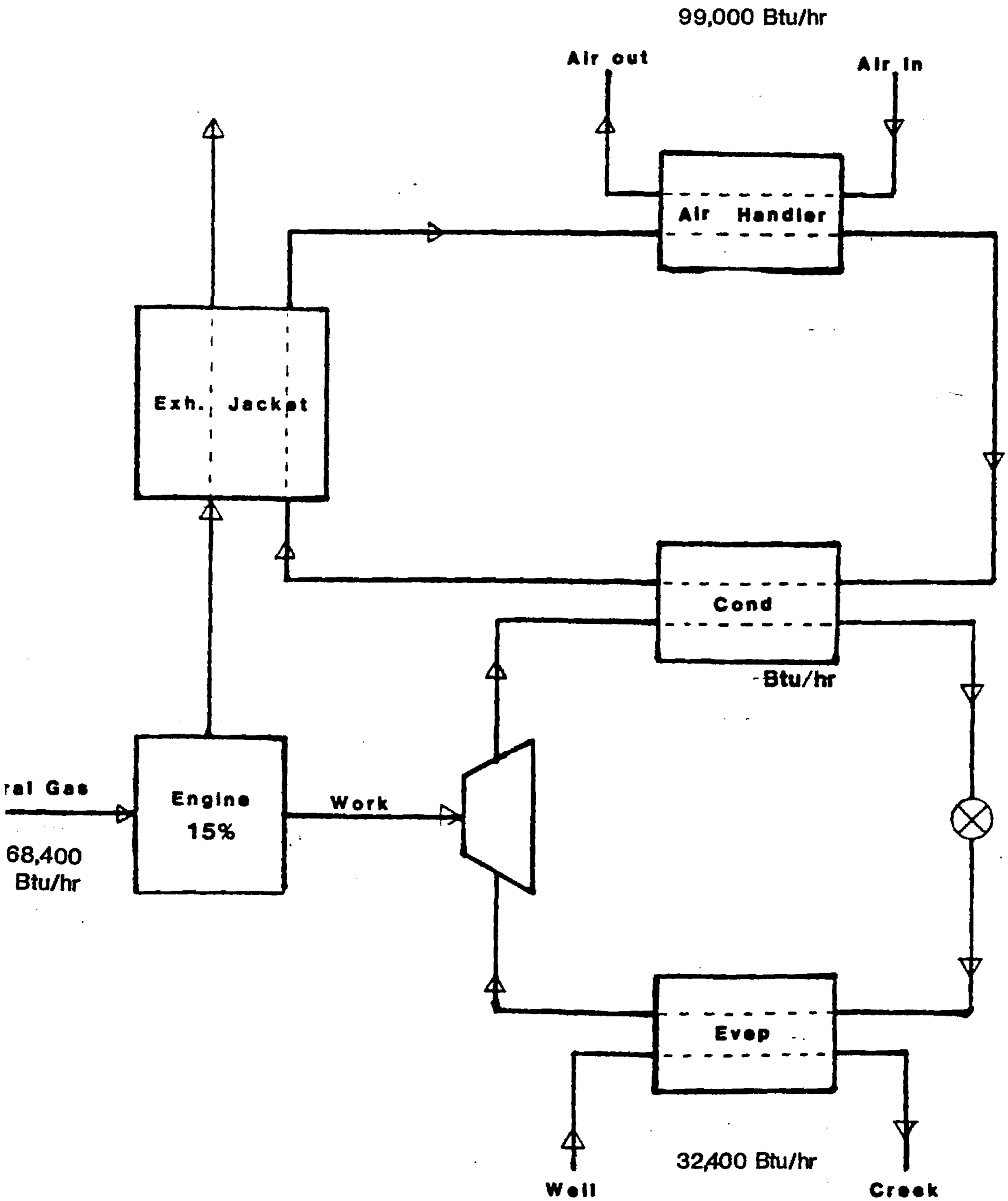

HEATING C.O.P. : 1.45

FIGURE 9: SEASONAL SYSTEM COOLING PERFORMANCE

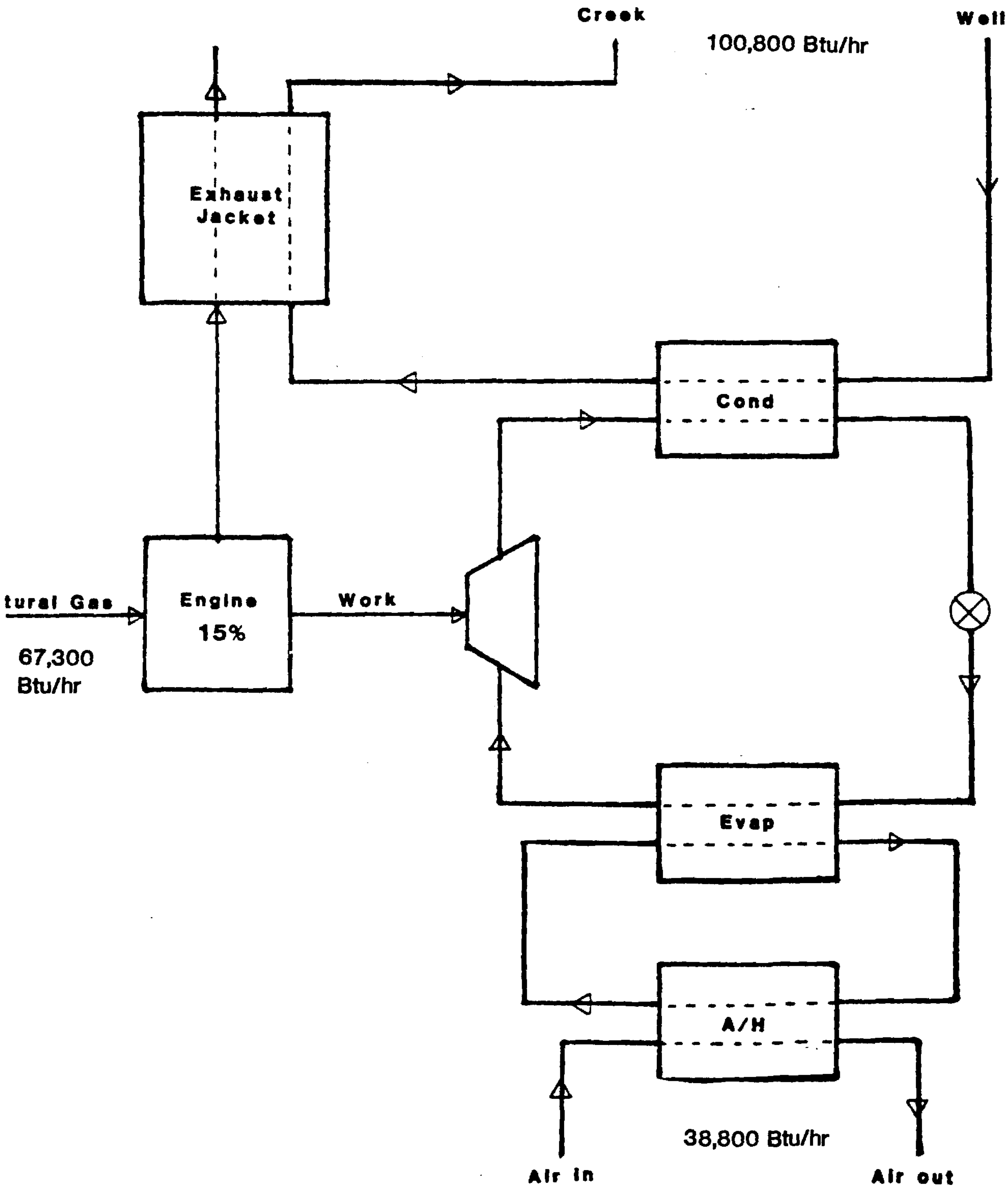

COOLING C.O.P. : 0.58

Engine/Compressor Performance

Data was taken from the experimental heat pump system for the purpose of determining engine/compressor performance (gas input rate, condenser and evaporator heat rates, and the heat recovery rate) as functions of the condenser and evaporator refrigerant temperatures. With the engine speed held constant, the gas input rate and condenser and evaporator heat rates are uniquely determined by the two refrigerant temperatures. The heat recovery rate is additionally dependent upon the variable water temperature and flow rate at the inlet to the exhaust heat exchanger.

Four operating conditions, each specified by a condenser refrigerant temperature and an evaporator refrigerant temperature, were used to obtain the experimental data. The operating conditions, listed in Table 4, were chosen near lower and upper temperature extremes in order to obtain a good representation over the range of experimental operating conditions. In order to achieve steady-state for each of the specified operating conditions, three different operating modes were required as indicated in Table 4.

The water temperature at the inlet to the exhaust heat exchanger (and, therefore, the heat recovery rate) varies with the operating mode. During normal heating operation, this temperature would be constant, yielding a constant exhaust temperature of approximately 130°F at the heat exchanger outlet.

Therefore, the measured heat recovery rate was corrected by calculating the change in exhaust heat recovery due to fixing the final exhaust temperature at 130°F.

A total of forty tests (ten for each of the four operating conditions) were conducted at a constant engine speed of 1200 rpm. After establishing steady-state (as determined by continuous monitoring of water temperatures in the condenser and evaporator loops), the gas input rate, condenser and evaporator heat rates, and heat recovery rate were computed for one-minute tests and logged by the APPLE/ ISAAC instrumentation system. For each set of operating conditions, the data was averaged over ten tests, and the results are given in Table 5. Included are the mean values and estimated true population standard deviations for the measured gas input rate, the measured condenser and evaporator heat rates, the measured heat recovery rate, and the corrected heat recovery rate.

The data presented in Table 5 provides an indication of the dependence of engine/compressor performance and the heat recovery rate on the condenser and evaporator refrigerant temperatures. For a change in one of the refrigerant temperatures with the other held constant, a change is estimated for the gas input rate, condenser and evaporator heat rates, and the heat recovery rate. The question was raised as to whether these changes are actual, or due to random error in the experimental data. A statistical analysis was performed to determine confidence intervals for changes in the data (dependent variables) resulting from changes in the refrigerant temperatures (independent variables).

$$\text{Confidence Interval} = \bar{X}_2 - \bar{X}_1 \pm t_p \left[\frac{(n+m)(n\sigma_1^2+m\sigma_2^2)}{nm(n+m-2)} \right]$$

where $\bar{X}_1$ and $\bar{X}_2$ are the averaged dependent variables involved in the change of one of the independent variables, σ_1 and σ_2 are the estimated true population standard deviations for the dependent variables, and n and m are the numbers of dependent variable data points. The variable t_p is tabulated[6] as a function of the degrees of freedom (n+m-2) and the confidence coefficient. For this data, the degrees of freedom are 18, and for a confidence of 90%, $t_p = 1.734$; 95%, $t_p = 2.101$; and 99%, $t_p = 2.878$. Confidence intervals for the changes in data, resulting from the increase in condenser refrigerant temperature are listed in Table 6. The negative signs on some of the interval bounds indicate that those rates decreased when the condenser temperature was increased. Confidence intervals for the changes in data resulting from the increase in evaporator refrigerant temperature are given in Table 7.

A good degree of confidence is indicated when the intervals are small relative to the magnitudes of their bounds. A review of Table 5 and 6 indicates a good degree of confidence in the change in condenser and evaporator heat rates for a change in either of the refrigerant temperatures. This implies that the rate changes are more likely due to changes in operating conditions than to random error in the data. On the other hand, little confidence can be placed in the change in heat recovery rate accompanying changes in either of the refrigerant temperatures. For instance, it is not known with a 99% certainty whether the heat recovery rate increases or decreases when the condenser temperature is increased.

A multiple variable, linear regression analysis program, available through an APPLE computer software package, was used to determine a linear relationship between the heat pump performance and the condenser and evaporator refrigerant temperatures. Data from all forty tests was used for the analysis. The results are included in Table 8 along with statistical analysis of the curve fits. These results are useful in design optimization of I.C. engine heat pumps.

System Steady State Performance

The computer data acquisition system supplied data from startup to establishment of steady state conditions for both the heating and cooling modes. Steady state was established in 20 to 30 minutes in the cooling mode and 30 to 40 minutes in the heating mode. The warmup period was longer for the heating cycle due to the higher equilibrium temperature in the hot water loop (about 140°F vs. 70°F). The speed was held constant at 1200 rpm.

Table 9 shows the steady state values for the temperatures, energy flow rates, and COPH's. The temperature numbers are labeled on the system schematic in Figure 5. In the heating mode, 57% of the heat was produced by the condenser, 41% from the engine cooling jacket and integral exhaust manifold/HX, and 2% from the external exhaust heat exchanger. The evaporator and condenser temperatures were about 31^{o}F and 132^{o}F, respectively. Only 1 1/2% of the gas input plus evaporator input energy is unaccounted for. The only significant loss would be in the exhaust gases which are at 117^{o}F. The accuracy of this "lost" heat number is very low due to accumulative errors of the numbers totaled to derive it.

In the cooling mode, 59% of the rejected heat comes from the condenser, 39% from the engine cooling jacket and exhaust manifold, with 2% coming from the external exhaust heat exchanger. The evaporator and condenser temperatures were approximately 33^{o}F and 88^{o}F, respectively. Only 3% of the total gas and evaporator energy input is unaccounted for. Again, the accuracy of this number is low, but with a 75^{o}F final exhaust temperature and insulated heat pump package, the unmeasured energy flow should be small.

The larger fraction of heat coming from the condenser in the cooling mode is due to the lower condenser temperature and pressure, yielding both a higher refrigerant mass flow and a lower engine loading.

Table 4. Steady-State Operating Conditions

Operating Condition	T_{Evap}(°F)	T_{Cond}(°F)	Operating Mode
1	27.5	86.9	3*
2	27.5	145.4	4
3	14.0	95.0	1
4	39.2	95.0	3*

*Mode 3 was modified by opening valve M-5 and placing valve A-1 in position "a".

Table 5. Averaged Experimental Data

Operating Condition	T_{Evap} (°F)	T_{Cond} (°F)	$\bar{Q}_{Gas}\,(\frac{Btu}{hr})$ [$\sigma(\frac{Btu}{hr})$]	$\bar{Q}_{Cond}\,(\frac{Btu}{hr})$ [$\sigma(\frac{Btu}{hr})$]	$\bar{Q}_{Evap}\,(\frac{Btu}{hr})$ [$\sigma(\frac{Btu}{hr})$]	$\bar{Q}_{Rec}\,(\frac{Btu}{hr})$ [$\sigma(\frac{Btu}{hr})$]	$\bar{Q}_{Rec}^{Corr}\,(\frac{Btu}{hr})$ [$\sigma(\frac{Btu}{hr})$]
1	27.5	86.9	76950 [0]	67384 [1871]	49804 [957]	55374 [3041]	49813 [3041]
2	27.5	145.4	84645 [1539]	49639 [863]	29781 [363]	47261 [1127]	47261 [1127]
3	14.0	95.0	70178 [1231]	43492 [2424]	32438 [439]	51791 [3396]	47176 [3396]
4	39.2	95.0	79412 [1231]	82614 [1821]	61362 [1520]	57706 [1488]	51968 [1488]

Table 6. Confidence Intervals for Increase in Condenser Temperature

	Confidence Coefficient		
	90%	95%	99%
$\Delta\bar{\dot{Q}}_{Gas}(\frac{Btu}{hr})$	[6805;8585]	[6617;8773]	[6219;9171]
$\Delta\bar{\dot{Q}}_{Cond}(\frac{Btu}{hr})$	[-18936;-16554]	[-19188;-16302]	[-19722;-15768]
$\Delta\bar{\dot{Q}}_{Evap}(\frac{Btu}{hr})$	[-20615;-19431]	[-20740;-19306]	[-21005;-19041]
$\Delta\bar{\dot{Q}}_{Rec}(\frac{Btu}{hr})$	[-4426;-677]	[-4823;-281]	[-5663;559]

Table 7. Confidence Intervals for Increase in Evaporator Temperature

	Confidence Coefficient 90%	95%	99%
$\Delta\bar{\dot{Q}}_{Gas}(\frac{Btu}{hr})$	[8228;10740]	[8015;10453]	[7564;10904]
$\Delta\bar{\dot{Q}}_{Cond}(\frac{Btu}{hr})$	[37370;40874]	[36999;41245]	[36213;42031]
$\Delta\bar{\dot{Q}}_{Evap}(\frac{Btu}{hr})$	[28010;29838]	[27816;30032]	[27406;30442]
$\Delta\bar{\dot{Q}}_{Rec}(\frac{Btu}{hr})$	[2649;6935]	[2195;7389]	[1235;8349]

Table 8. Results of Multiple Variable, Linear Regression Analysis

$\dot{Q}_{gas}(\frac{Btu}{hr}) = 372.91T_{Evap} + 159.80T_{Cond} + 50838$ *
Coefficient of Determination (R^2) = .89434
Coefficient of Multiple Correlation = .94570
Standard Error of Estimate ($\frac{Btu}{hr}$) = 1801.6
$\dot{Q}_{Cond}(\frac{Btu}{hr}) = 1553.5T_{Evap} - 298.68T_{Cond} + 50292$ *
Coefficient of Determination (R^2) = .98577
Coefficient of Multiple Correlation = .99286
Standard Error of Estimate ($\frac{Btu}{hr}$) = 1918.3
$\dot{Q}_{Evap}(\frac{Btu}{hr}) = 1145.8T_{Evap} - 351.09T_{Cond} + 49420$ *
Coefficient of Determination (R^2) = .99377
Coefficient of Multiple Correlation = .99688
Standard Error of Estimate ($\frac{Btu}{hr}$) = 1064.6
$\dot{Q}_{Rec}(\frac{Btu}{hr}) = 189.52T_{Evap} - 46.400T_{Cond} + 48827$ *
Coefficient of Determination (R^2) = .39396
Coefficient of Multiple Correlation = .62766
Standard Error of Estimate ($\frac{Btu}{hr}$) = 2558.6

*T_{Evap} and T_{Cond} in °F

TABLE 9
Steady State Performance

Temperatures (°F)	Heating Mode	Cooling Mode
T_1 - Evaporator water inlet	57.5	52.2
T_2 - Evaporator water outlet	43.3	42.3
T_6 - External exhaust HX water inlet	113.2	60.7
T_3 - Condenser water inlet	113.7	61.2
T_4 - Engine water inlet	129.4	77.6
T_5 - Engine water outlet	140.7	88.3
T_8 - Exhaust gas outlet	117.8	74.7
T_9 - A/H air inlet	70.9	77.5
T_{10} - A/H air outlet	108.9	59.0
Energy Flows (Btu/hr)		
Gas consumption	68,700	67,700
Engine & exhaust manifold recovery	40,100	40,600
External exhaust HX recovery	1,800	1,900
Condensor heating	55,700	62,300
Total heating	97,600	104,800
Evaporator Cooling	30,400	40,700
COPH's		
Heating	1.42	
Cooling		0.60

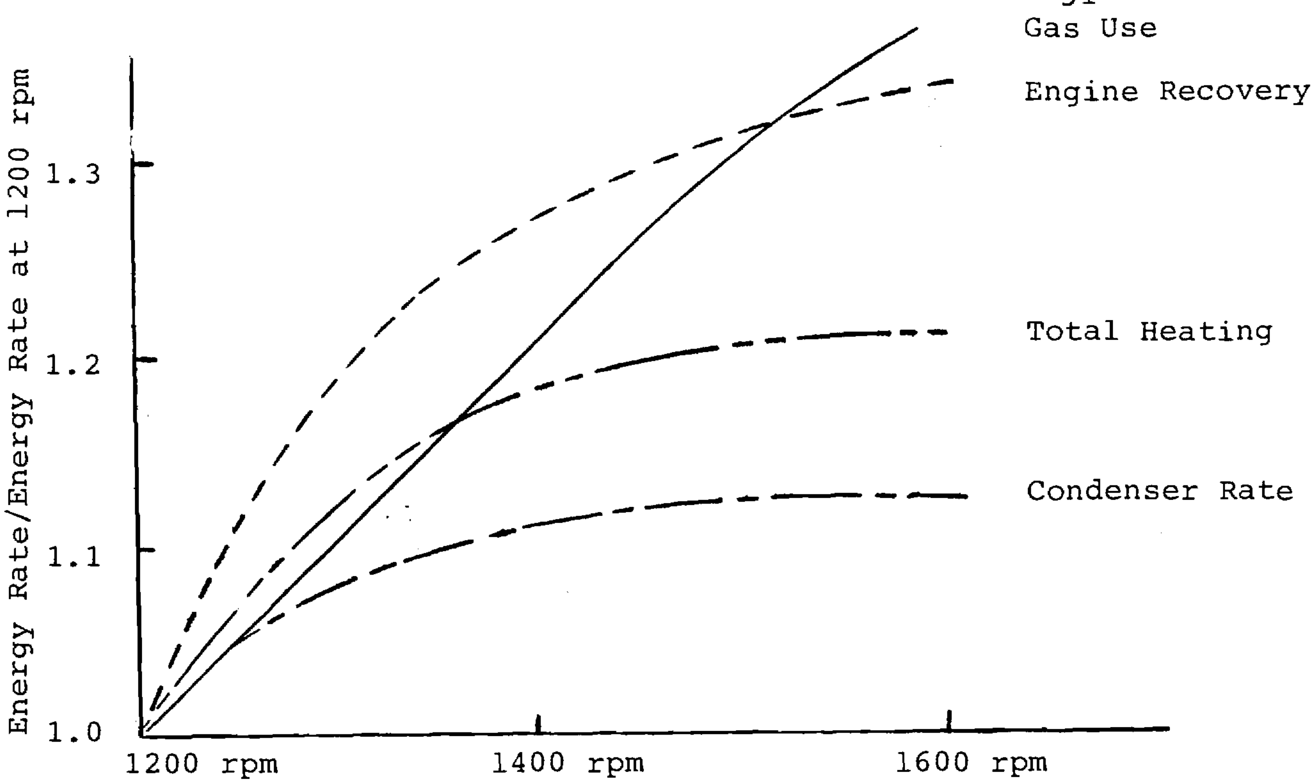

Figure 10. Heat Pump Energy Rates vs. Speed

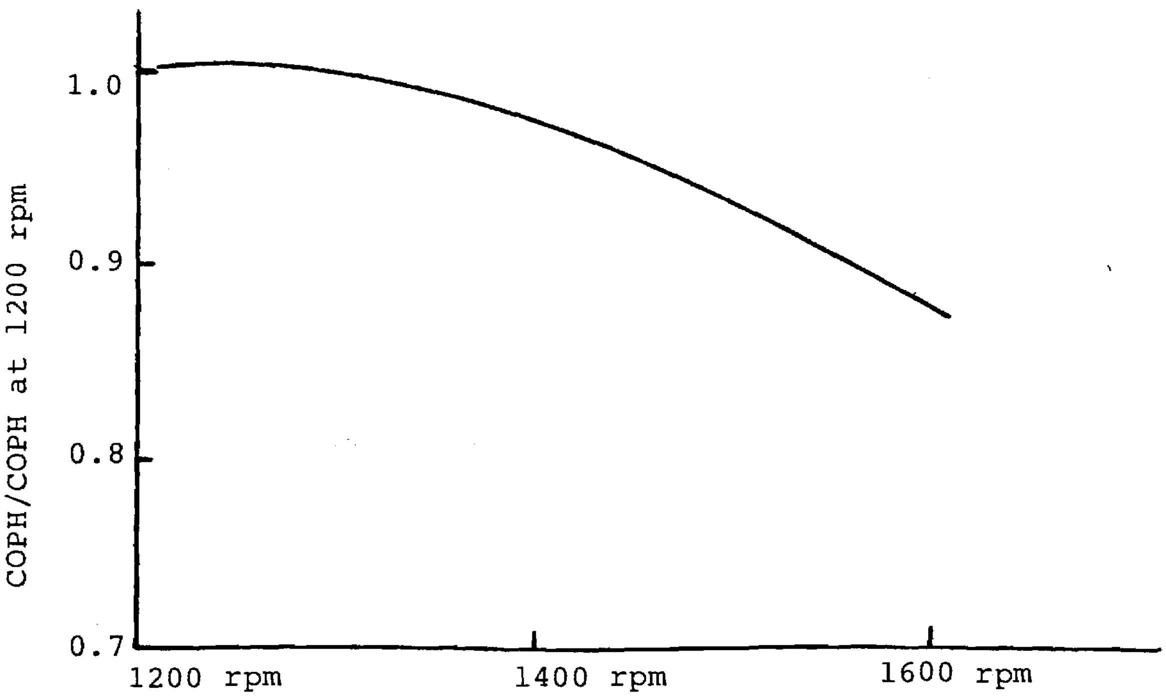

Figure 11. Heat Pump Heating COP vs. Speed

because the return water temperature from the air handler was driven up as a higher rate was put through the air-water coil. The well water temperature supplying the evaporator is of course constant with varying speed. These speed effects would not be as large with an air-to-air system without the additional water heat exchange process.

Figure 11 shows the resulting COPH for the varying speed. The efficiency is seen to decrease by about 15%, while the total heating rate increases by just over 20%, for a 25% speed increase. Again, it should be noted that the water-to-water heat pump will show larger efficiency penalties with increasing speed than does an air-to-air system.

Cycling Effects

The effect of on/off cycling of the heat pump in its performance was studied two ways. First, run-by-run data was accumulated by the computer data acquisition system. It printed out the average energy flow rates and COP's for each on-cycle, along with that cycle's on-time and prior off-time. Statistical analysis was carried out on this data to determine the correlation of the average cycle performance as a function of the cycle's on-time and the prior off-time. No significant dependence of any of the variables was found on these cycle times.

Due to this unexpected result, a cycling test was run which was patterned after the U.S. Department of Energy's test procedure for measuring electric air conditioner and electric heat pump cycling effects, published January 1, 1982, (Chapter 2, Title 10, Subpart B, Appendix M). In this test a 30 minute run is made to establish steady-state conditions, followed by a 30 minute period during which the steady-state performance is measured. During the next 30 minute period, the heat pump is off 24 minutes and then turned on for 6 minutes. This 24 minutes off, 6 minutes on cycle is repeated twice with the last 6 minute cycle being used to measure the performance during cycling relative to the initial steady-state values.

A DOE cycling degradation coefficient, C_D, is defined as:

$$C_D = 1 - \frac{COP_{cyc}}{COP_{ss}} = 1 - \frac{Q_{cyc}}{Q_{ss}}$$

where $(\ )_{cyc}$ indicates the values for the last 6 minute on cycle and $(\ )_{ss}$ is the 30 minute steady-state measured values. In these tests the C_D repeatedly came out negative, indicating and improvement in efficiency during cycling.

This unusual result is shown to be due to the "spin down" cycle which extracts the engine/condenser heat for 6 minutes following an on-cycle. This spin down reduces the hot water temperature from about 140°F to less than 110°F. Since the condenser is in the same hot water loop with the engine and exhaust, this significantly reduces the average condenser temperature during cycling compared with steady-state, while still extracting all the engine heat. Accessory energy is also increased.

This cycling effect may not be the same with an air-to-air system, since the I.C. engine heat pump condenser temperature would not be tied to the engine temperature. However, since approximately half of the total heat comes from the engine, cycling effects of an I.C. engine heat pump would be expected to be substantially less than an electric heat pump, particularly if a spin down cycle is used.

Reliability and Maintenance

One of the goals for the I.C. engine heat pump is to have a maintenance interval greater than once annually. This goal was exceeded by this experimental system in that no scheduled or unscheduled maintenance was carried out during the over 200 running hours, except for the installation of an oil sealing gasket on a cover plate on the side of the engine. No oil changes, spark plug replacement, timing adjustment, or any other maintenance has been required or performed. Spark plug gap is still under 0.040 inch due to special tip materials.

Oil analysis has been carried out, showing at the 1750 hour point, that the oil was still completely serviceable. The analysis at 1750 hours is shown in Table 10. The 15 quart capacity is continually recirculated.

Reliability has been nearly 100%, except for several increasingly frequent occasions when the engine failed to start during the first 5 second fixed starting period. This failure occurs generally after the heat pump has not run for a long period of time. After five seconds, the starter is

TABLE 10: Oil Analysis

WEAR CHECK

ENGINE AND OIL CONDITION ANALYSIS REPORT

Spectro/Metrics, Inc.
35 Executive Park Drive, N.E.
Atlanta, Georgia 30329
(404) 321-7909

': FORD MODEL: 2270 FLEET/UNIT #: 1 NATURAL GAS

SAMPLE DATA	WEAR METALS						SILICON	ADDITIVES				CONTAMINANTS				VISC.	TBN
	ALUMINUM	CHROMIUM	COPPER	IRON	LEAD	TIN		MAGNESIUM	MOLY	BORON	SODIUM	WATER (%)	GLYCOL	DIELECTRIC	FUEL (%)		
	PISTONS BEARINGS	RINGS	BEARINGS	CYLINDER RINGS CRANKSH CAMSH	GASOLINE ADDITIVE – DIESEL BEARINGS	BEARINGS	DIRT (ADDITIVE)	ADDITIVE (HOUSING)	ADDITIVE (RINGS)	ADDITIVE (COOLANT)	ADDITIVE (COOLANT)	CONDENSATION (COOLANT)	ANTI FREEZE	SOLIDS CARBON		SAE	ALKALINE RESERVE
te pled 10-2-82 le # 14026	4.6 N	5.1 N	22 N	72 N	6.2 N	9.2 N	13 N	805 N	2.7 N	13 N	18 N	-.05 N	NEG N	4 N	0 N	31	

2 # 214058
les Hrs 1750
rs Since change 1750
rs since change 1750

ENGINE WEAR RATES AND CONTAMINANT LEVELS SATISFACTORY. OIL STILL SERVICEABLE. RESAMPLE NEXT SERVICE INTERVAL TO MONITOR AND ESTABLISH WEAR TREND. (NO PREVIOUS RECORD WITH THIS UNIT I.D. PLEASE PROVIDE LAST LAB NUMBER.) -ANALYST RT

END: Normal, Abnormal, Severe. "+" means greater than, "–" means less than.

DR. SAM. V. SHELTON
SCHOOL OF MECHANICAL ENG.
GEORGIA TECH
ATLANTA, GA 30332

LAST OVERHAUL:
SYSTEM CAPACITY: 15 QTS.
OIL MAKE & TYPE: ?
HISTORY & REMARKS:

DiesGasNat 79

SHEATL 1

A MEMBER OF THE SPECTROMETRIC OIL ANALYSIS LABORATORY ASSOCIATION deactivated; if oil pressure is not sensed 10 seconds after starter initiation, the controls shut the unit down on default. In almost every start failure, a manual reset to allow a second try was successful. A third and four try was required in isolated instances. This problem could be overcome by using controls to reinitiate the start cycle automatically.

Noise Levels

Sound levels of the unit have been measured using a an A weighting scale. Inside the furnace room the levels were as follows for individual components running and with the total system running:

Background	-	57 dBA
Air Handler Only	-	61 dBA
Water Pump Only	-	57 dBA
Heat Pump Only	-	62 dBA
Total System	-	63 dBA

Sound levels were also measured outside at a 6 foot distance from the exhaust outlet. The outlet is 8 inches above a concrete slab and 6 inches from a 8 foot high concrete block wall. The second level at a distance 6 feet from this wall is 60 dBA.

Electrical Accessory Power

The electrical accessories with this gas heat pump are 1) a 1/2 hp A/H fan drive; 2) two 1/5 hp closed loop water circulating pump drives (only one is on in any mole); 3) a 1/2 hp well water pump drive, and 4) a lead acid battery charger. The battery charger draws about 10 watts and is not significant. The kilowatt draw of the other accessories are:

Fan	-	0.73 kw
Well Pump	-	0.61
Circulating Pump (1)	-	0.24
Total	-	1.58 kw

The 1.6 kw power is drawn during the heat pump operating hours. In addition, for 6 minutes after the heat pump is shut down, the fan and one circulating pump operate, drawing a total of 1.0 kw.

A separate kilowatt hour meter accumulated the electrical consumption of these accessories. The average kwhr consumption was 1.91 kwhr per hour of heat pump running time. This average compares with the gas consumption of 0.67 therms per hour. At a 3.5 ratio for electrical energy cost to gas energy cost (6.5 ¢/kwhr and 55 ¢/therm), the electrical accessories energy cost is 25% of the total heat pump system operating cost.

Performance Improvements

Changes for improved efficiency performance would be to retrofit the heat pump with a smaller displacement engine. The present Ford 227E 1600 cc engine is operating at 25% of its rated full load. Figure 12 is a plot of engine efficiency vs. % load with engine speed as a parameter. From this figure it can be seen that at 25% loading and 1200 rpm, the engine's thermal efficiency is about 16%. If this engine were replaced by a Ford 2271E 1100 cc engine, the loading would increase to approximately 36%. From Figure 12, this increased load at 1200 rpm would result in a thermal efficiency of about 19%. This change alone would yield a 25% improvement in cooling COP and about a 10% improvement in heating COP.

Figure 12: Engine Efficiency vs Load

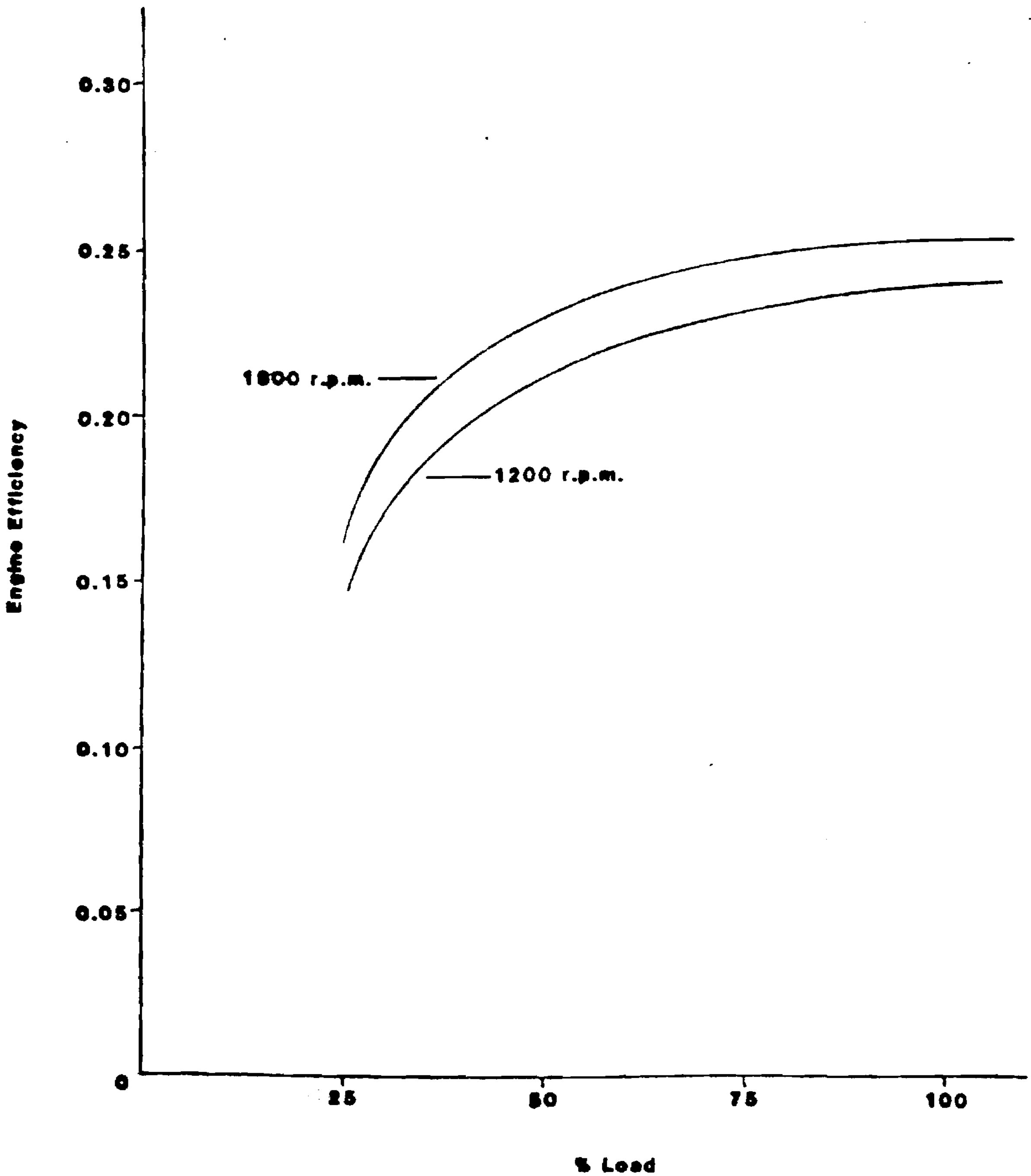

SECTION V

AIR-TO-AIR I.C. ENGINE HEAT PUMP ANALYSIS

Introduction

The water-to-water heat pump tested gave information on the critical engine/compressor subcomponent in terms of the physical characteristics, maintenance, noise, and reliability of I.C. engine heat pumps. However, the efficiency information is not directly applicable to air-to-air heat pumps. Even so, the experimental data taken on just the engine/compressor yielding energy rates and efficiencies for varying condenser and evaporator pressures makes it possible to calculate accurately the performance of the same engine/compressor operating with a given size of air condenser and evaporator coils.

The proposed system model diagram is given in Figure 13. Indoor and outdoor air are used as the heat source/sink for the vapor-compression cycle heat pump. Heat is removed from the source and rejected to the sink via two refrigerant-air heat exchanger coils. These coils are fixed in position, but the reversing valve makes possible a change in the direction of refrigerant flow to and from the compressor. The direction of refrigerant flow defines which coil is the condenser and which is the evaporator, and thereby defines the direction of heat flow.

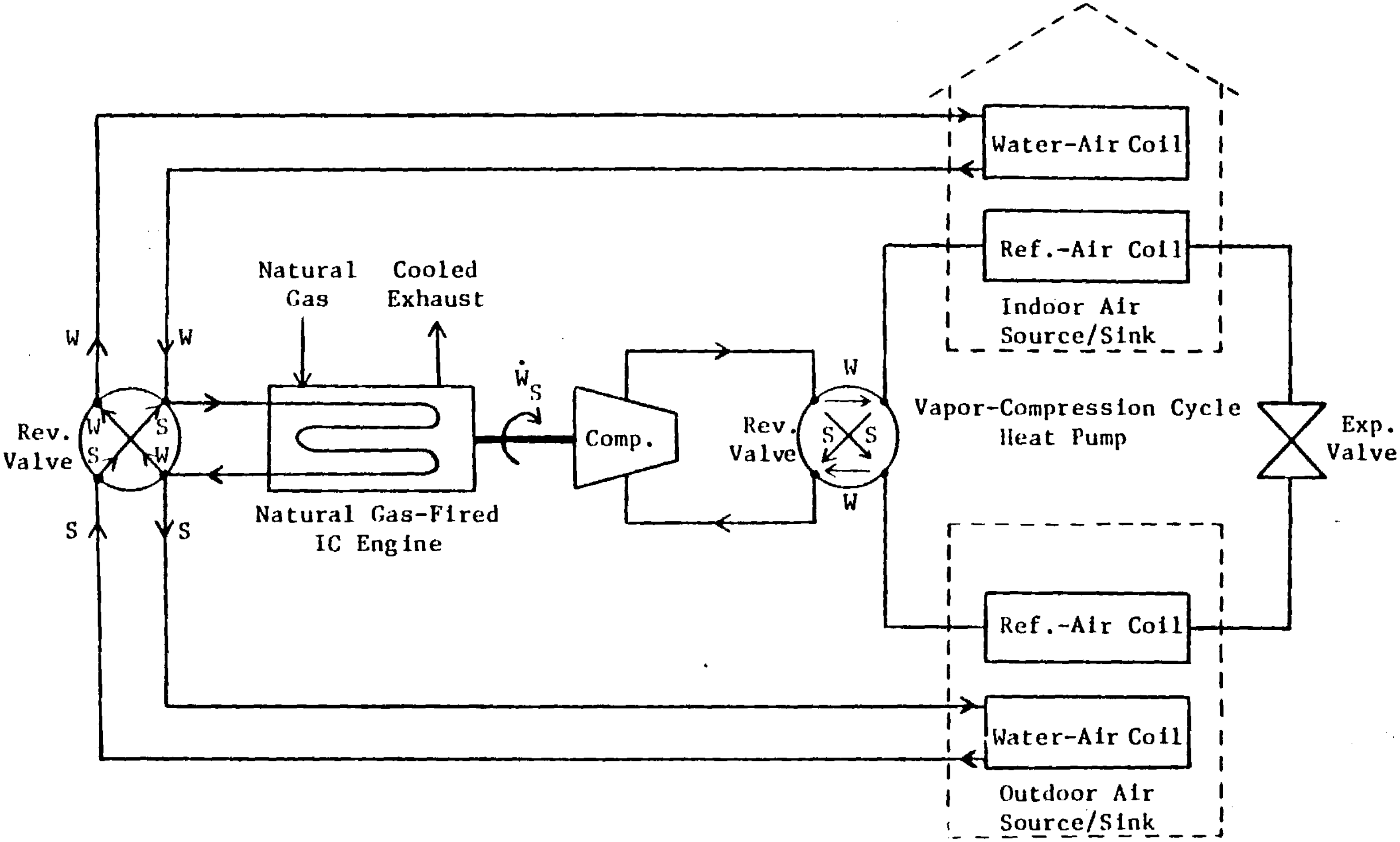

Figure 13: Air-to-Air Heat Pump Model Diagram

Water is used as a transger medium to remove combustion waste heat from the natural gas-fired I.C. engine. Heat removed from the engine block and exhaust gas is rejected to the heat sink via one of two water-air heat exchanger coils. A reversing valve is used to circulate water from the engine to the indoor coil (for simultaneous engine cooling and space heating) or to the outdoor coil (for engine cooling during space cooling).

An analytical model optimizes the air coils for the engine/compressor tested. The engine/compressor performance and heat recovery data are taken as input from the experimental data shown in Section IV. The operating performance for space heating and cooling is determined as a function of the refrigerant-air coil air flow rates and heat exchanger UA's (overall heat transfer coefficient times total wall surface area) for a range of outdoor air temperatures. The annual gas consumption required for space heating and cooling is then calculated for fixed residential thermal characteristics (UA - 680 Btu/hr-^{o}F) and weather data using the "bin" method of analysis. From this data, the indoor vs. outdoor refrigerant coil UA is optimized. The annual performance for varying total indoor plus outdoor coil UA is then calculated so that the performance of this engine/compressor subcomponent, operating in an air-to-air system, may be determined for a given total air coil size and cost.

Analysis

Energy balances on the air flowing through the condenser and evaporator coils produce these fundamental equations:

$$\dot{Q}_{Cond} = (\dot{m}C_p)_{Cond}(T_o - T_i)_{Cond}$$

$$\dot{Q}_{Evap} = (\dot{m}C_p)_{Evap}(T_i - T_o)_{Evap}$$

where the C_p's have been assumed constant and the temperature subscripts, i and o, refer to the air inlet and outlet of the coils. Another set of fundamental equations is obtained from counter-flow heat exchanger analysis:

$$\dot{Q}_{Cond} = [UA(LMTD)]_{Cond} = UA \left[\frac{T_o - T_i}{\ln \frac{T_{Cond} - T_i}{T_{Cond} - T_o}} \right]_{Cond}$$

$$\dot{Q}_{Evap} = [UA(LMTD)]_{Evap} = UA \left[\frac{T_i - T_o}{\ln \frac{T_i - T_{Evap}}{T_o - T_{Evap}}} \right]_{Evap}$$

where LMTD is the logarithmic mean temperature difference between the refrigerant and the air.

The heating and cooling requirements of the residential structure define the house load, from which the annual gas consumption can be determined. When the outdoor air temperature (or ambient air temperature) is below the desired indoor air temperature, the required heating rate is:

$$\dot{Q}_{HL} = (UA)_{House}(T_i - T_{amb})_{Heating}$$

Similarly, when the ambient air temperature is above the desired indoor air temperature, the required cooling rate is:

$$\dot{Q}_{CL} = (UA)_{House}(T_{amb} - T_i)_{Cooling}$$

These equations assume that the house model UA is independent of the ambient air temperature. In a study by the National Bureau of Standards, the historical energy consumption for heating and cooling was correlated with weather data, and good agreement was obtained using a constant house model UA. The bin method is used to estimate the annual heating and cooling loads from the last two equations.

The above equations represent the analytical heat pump model. Together, they comprise nine equations with unknowns. The unknowns are T_{Cond}, T_{Evap}, $T_{o_{Cond}}$, $T_{o_{Evap}}$, $\dot{Q}_{Cond}$, $\dot{Q}_{Evap}$, $\dot{Q}_{Rec}$, $\dot{Q}_{Gas}$, and Q_{Gas}^{Annual}. The remaining variables are input parameters. These include the house model UA and the condenser and evaporator coil inlet air temperatures, air flow rates, and UA's. For heating, $T_{i_{Cond}}$ is the desired indoor air temperature and $T_{i_{Evap}}$ is the outdoor air temperature. For cooling, the coils are reversed so that $T_{i_{Cond}}$ is the outdoor air temperature and $T_{i_{Evap}}$ is the desired indoor air temperature. In matrix form, these equations are easily solved (for a given set of input conditions) by Gauss elimination. If these calculations are performed at the median outdoor air temperature of each bin, the results can be used to determine the total annual gas consumption for heating and cooling of the residential structure.

A computer program was set up on an APPLE II computer to run through all of these calculations.

Input Parameter Considerations

The desired indoor air temperatures are chosen to be $68^{\circ}F$ for heating, and $76^{\circ}F$ for cooling, normal conditions for residential and small commercial establishments. The house model UA is taken from a heating and cooling load study on the Atlanta residence accommodating the experimental heat pump system. In that study, the UA was estimated at 680 Btu/hr-$^{\circ}F$ for both heating and cooling. The analytical heat pump design is optimized for this house load. The results are applicable to varying house loads if all system components are scaled proportionally.

In cooling, approximately 75% of the heat removed from the indoor air was assumed to be in the form of sensible heat. The remaining 25% was assumed to be latent heat due to dehumidification. To account for this dehumidification, the specific heat of the air flowing through the evaporator in the cooling mode is increased by a factor of 33% (25%/75%).

The indoor air flow rate is taken to be constant at 2500 cfm. This constant is necessary to ensure a high enough condenser air outlet temperature (105-115^{o}F) in the heating mode to prevent draft chill, and a low enough evaporator air outlet temperature (50-55^{o}F) in the cooling mode for sufficient dehumidification. The outdoor air flow rate is varied proportionally with the outdoor coil UA, such that the ratio of coil UA to volumetric flow rate for the outdoor coil is fixed coil is fixed at a typical value of 2.0 $\frac{\text{Btu/hr-}^{o}\text{F}}{\text{cfm}}$.

Three locations, Atlanta, Chicago, and Orlando, are chosen as having representative average, cold, and warm climates. The weather data (hours per year at each temperature bin) for these cities is found in U.S. Air Force Manual 88-29. In climates much colder than Chicago's, the heat pump may become less cost effective than direct heating systems because of the lower outdoor air (source) temperatures. In climates much warmer than Orlando's, the natural gas heat pump begins to lose its advantage over the electric heat pump because of the reduced heating hours.

Performance Optimization

The optimum heat pump performance for each city is determined by varying the ratio of indoor coil UA to outdoor coil UA. The optimum UA ratio, for a fixed total coil UA (indoor coil UA plus outdoor coil UA), or a fixed total coil cost, is defined as that yielding the lowest annual gas consumption. The annual gas consumption is calculated for total coil UA's of 2500, 5000, 10000, and 15000 Btu/hr-^{o}F at various UA ratios. The results of these calculations are graphed in Figures 14-16.

A curve is drawn through the optimum performance points in each of the graphs, and it is expected that the optimum performance for other values of total coil UA lies along these curves. The shape of these optimum performance curves is explained by considering that the total annual gas consumption is the sum of the annual gas consumption for both heating and cooling. The optimum UA ratio for heating decreases with increasing total coil UA, while that for cooling increases with increasing total coil UA. The degree of interaction between the two separate performance curves is dependent upon the heating and cooling load requirements. Listed in Table 11 are the heating and cooling loads for each city, along with the optimum heating, cooling, and overall UA ratios. In Chicago, where the heating load requirement is predominant, the optimum overall performance is essentially determined by the optimum heating performance. On the other hand, in Orlando, where the cooling load requirement is predominant, the optimum overall performance is essentially determined by the optimum cooling performance (more gas is required per Btu of cooling than per Btu of heating).

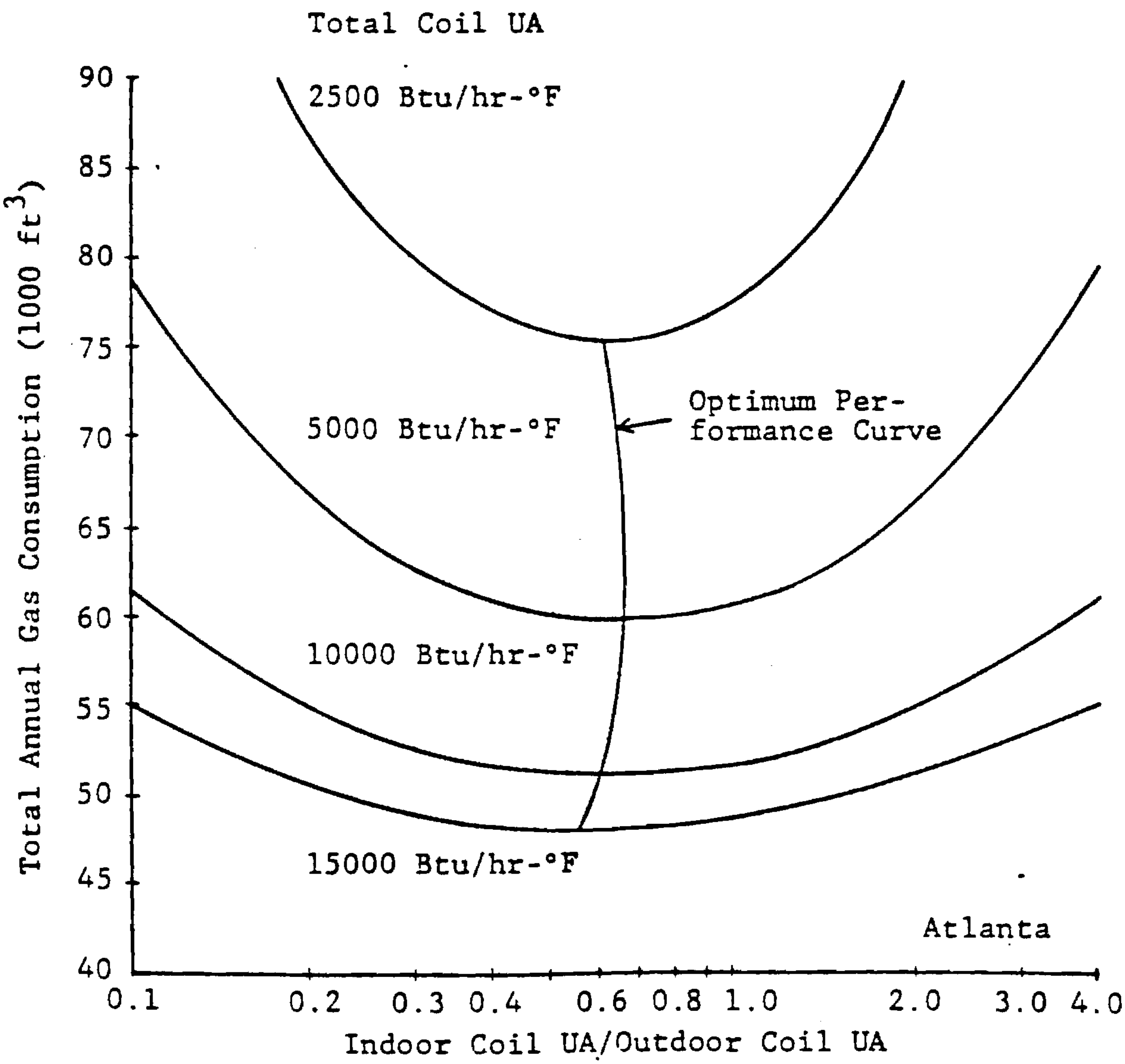

Figure 14: Annual Gas Consumption versus Coil UA Ratio, Atlanta

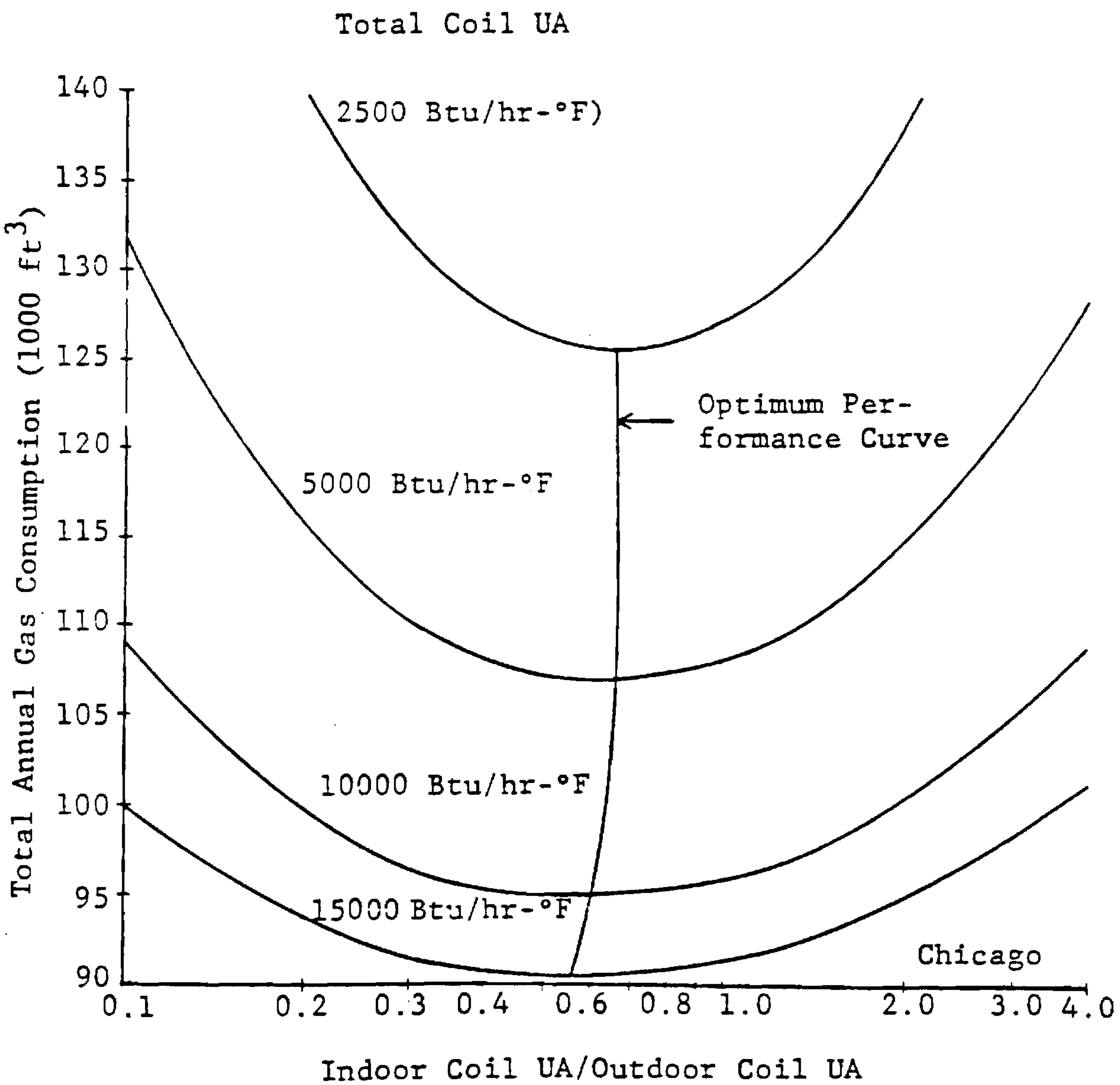

Figure 15: Annual Gas Consumption versus Coil UA Ratio, Chicago

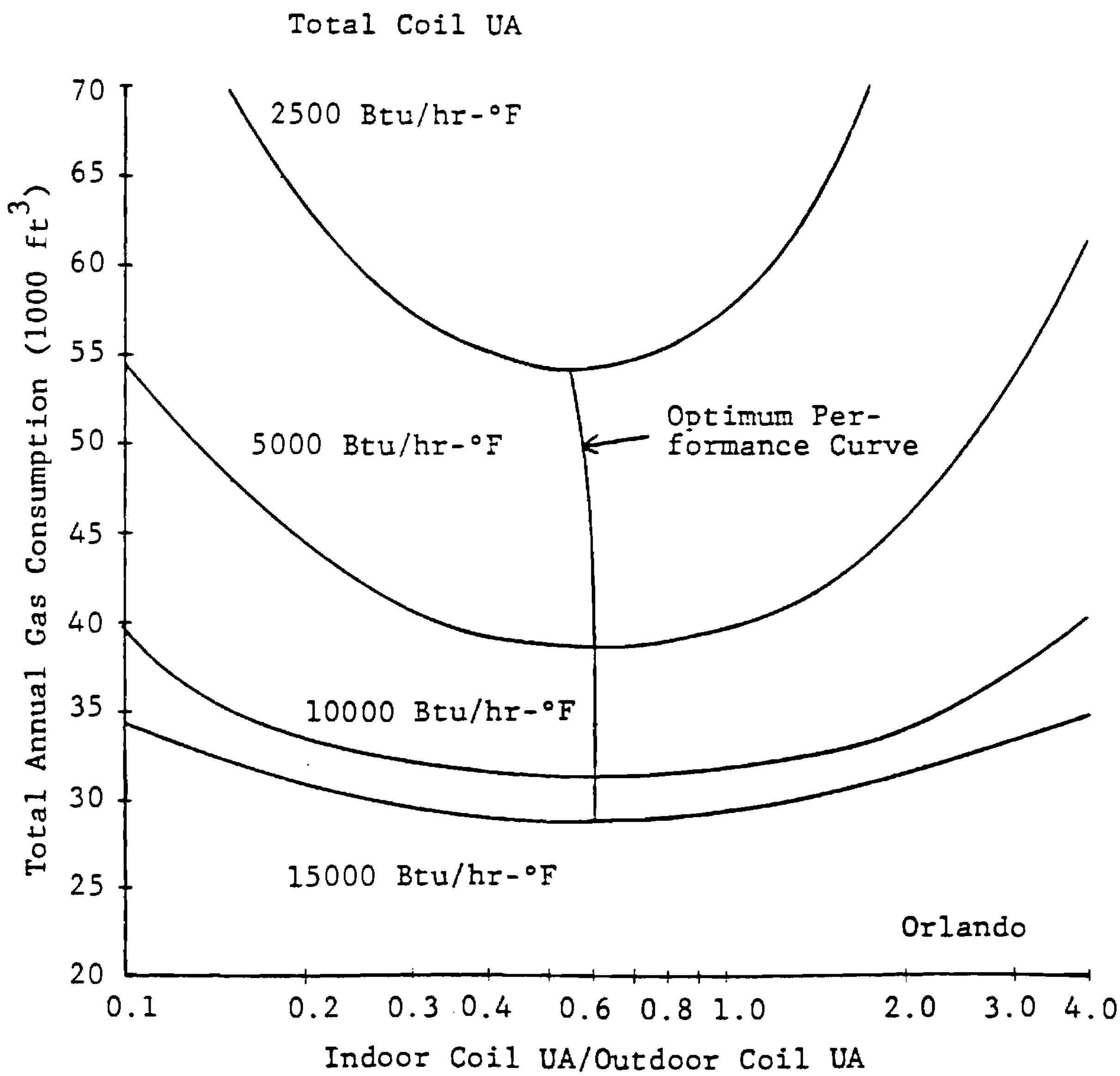

Figure 16: Annual Gas Consumption versus Coil UA Ratio, Orlando

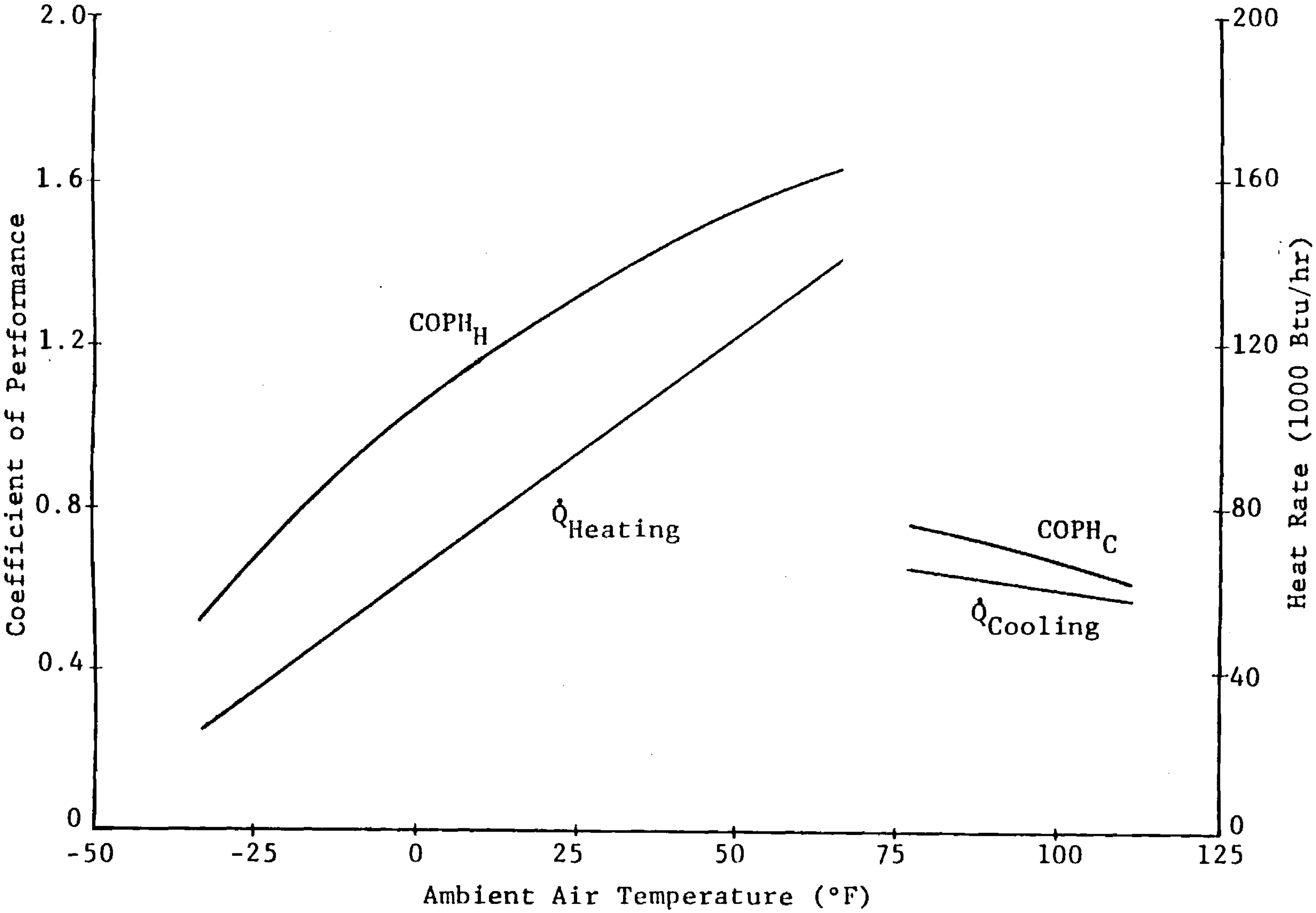

Figure 17: Heating and Cooling COP's and Rates at Optimum Performance for Total Coil UA = 10000 Btu/hr-°F

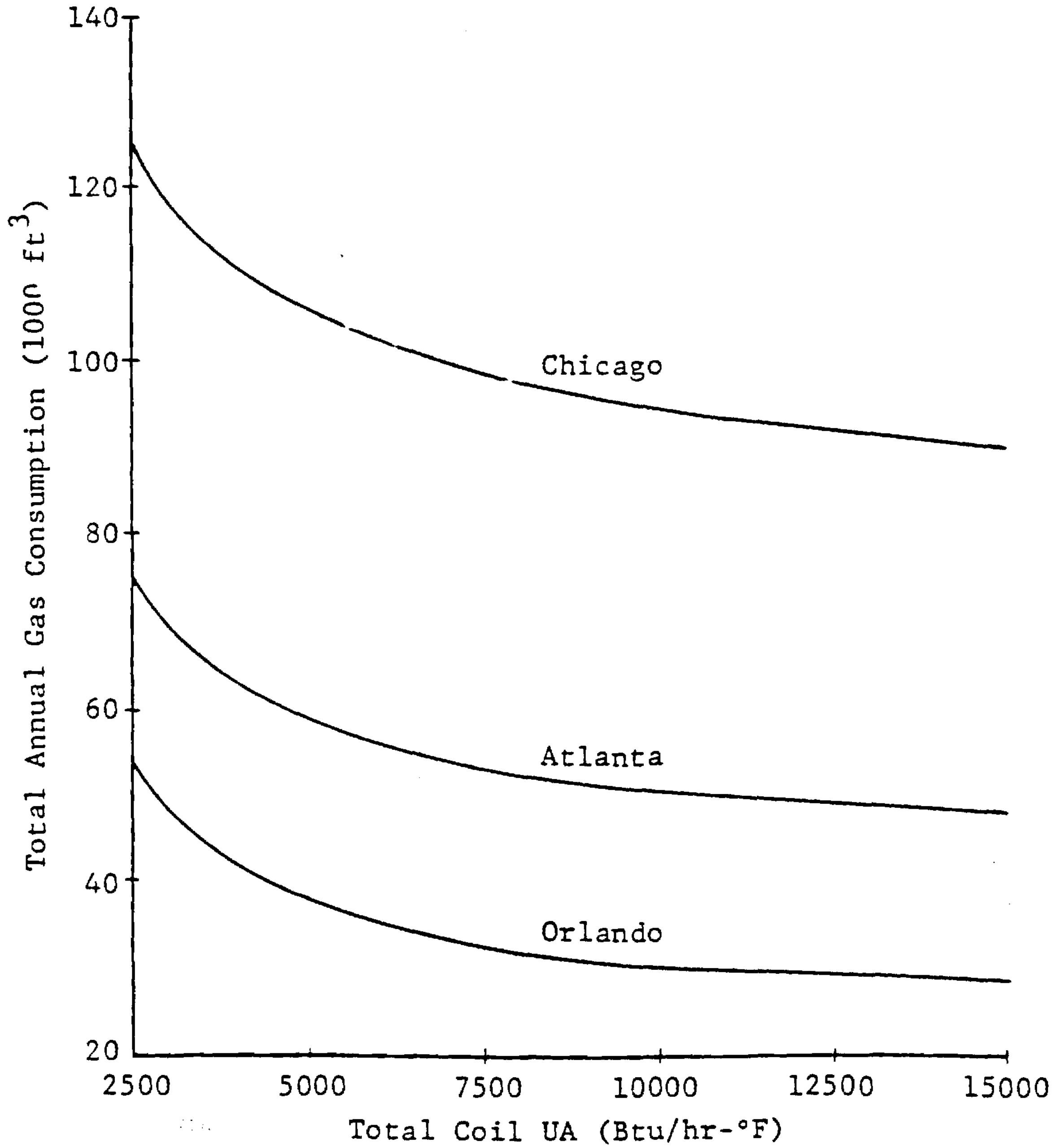

Figure 18: Annual Gas Consumption
at Optimum Performance

Table 11: Optimum Coil UA Ratios

City 1 - Annual Heating Load Requirement (Btu) 2 - Annual Cooling Load Requirement (Btu)	Total Coil UA (Btu/hr-°F)	Optimum UA Ratio $\left(\frac{\text{Indoor Coil UA}}{\text{Outdoor Coil UA}}\right)$		
		Heating	Cooling	Overall
Atlanta 1 - 59,866,860 2 - 8,255,880	5,000 10,000 15,000	0.65 0.60 0.55	0.60 0.60 0.60	0.65 0.60 0.55
Chicago 1 - 122,283,380 2 - 3,957,600	5,000 10,000 15,000	0.65 0.60 0.55	0.55 0.60 0.60	0.65 0.60 0.55
Orlando 1 - 20,342,880 2 - 13,623,460	5,000 10,000 15,000	0.70 0.60 0.60	0.60 0.60 0.60	0.60 0.60 0.60

Table 12: Annual Heating and Cooling COP's

at Optimum Performance

City	Total Coil UA (Btu/hr-°F)	$COPH_H$	$COPH_C$
Atlanta			
	5000	1.28	0.56
	10000	1.45	0.73
	15000	1.52	0.80
Chicago			
	5000	1.19	0.56
	10000	1.33	0.73
	15000	1.39	0.80
Orlando			
	5000	1.35	0.56
	10000	1.53	0.73
	15000	1.61	0.80

The heat pump design for optimum performance can be determined from Figures 14-16 for any total coil UA. For a total coil UA of 10000 Btu/hr-^{o}F, the optimum UA ratio is found to be 0.6 for Atlanta, Chicago, and Orlando. Then for optimum performance, the heat pump design would include an indoor coil with a UA of 3750 Btu/hr-^{o}F and an outdoor coil with a UA of 6250 Btu/hr-^{o}F. The heating and cooling COP's and rates at optimum performance for this design are plotted in Figure 17 as functions of the outdoor air temperature. Since the optimum UA ratio for a total coil UA of 10000 Btu/hr-^{o}F was found to be the same for Atlanta, Chicago, and Orlando, the curves in Figure 17 apply to all three cities. The annual heating and cooling COP's at optimum performance are presented in Table 12.

The annual gas consumption at optimum performance (from Figures 14-16) is given in Figure 18 as a function of total coil UA. This figure provides an indication of the savings in annual gas consumption that would be gained through the use of coils with a higher total UA. As one might expect, annual gas savings diminish with increasing increments of total coil UA.

Conclusions

This air-to-air I.C. engine heat pump analysis, using actual engine/compressor data, shows that the indoor coil UA should be about 0.6 of the outdoor coil UA and that for a total UA above 10000 Btu/hr-^{o}F, gas savings diminish rapidly. The heat pump size and coil UA should be proportional to the house thermal load, so that for a house half the size of that used, (UA - 680 Btu/hr-^{o}F), the total air coil UA should be scaled down to one-half as should all other components.

The resulting heating and cooling COP's for this particular package with a typical total inside plus outside coil UA of 10000 Btu/hr-^{o}F would then be:

	COP_H	COP_C
Atlanta	1.45	0.73
Chicago	1.33	0.73
Orlando	1.53	0.73

Since the engine used to obtain data for this analysis was only 25% loaded, a more closely matched engine/compressor (smaller engine) would improve these air-to-air heat pump COP's.

SECTION VI

CONCLUSIONS AND RECOMMENDATIONS

Introduction

The field testing and analysis of a natural gas I.C. engine heat pump has provided important information regarding the state of technology, potential performance, problem areas, and optimization of I.C. engine heat pumps. The most important of these conclusions is that several formerly perceived problem areas have been shown to be either non-existent or unimportant. Other conclusions are related to the performance of the tested unit, including seasonal performance, steady state performance, cycling effects, and speed variation effects. Design criteria for air-to-air I.C. engine heat pumps have also been developed. These specific conclusions and recommendations for further development of this concept are as follows.

Experimental Performance

The I.C. engine heat pump, with its Ford of Europe 1600 cc natural gas industrial engine, operated as a water-to-water heat pump to provide all space conditioning for an Atlanta residence over two heating and two cooling seasons. Measurement of its performance provided the following data. Speed was constant at 1200 rpm. The measured average winter seasonal energy rates were 68,400 Btu/hr for the gas use rate and 99,000 Btu/hr for the total heating rate, yielding a 1.47 seasonal heating COP. During the 561 hours of monitored summer cooling operation, the gas use rate was 67,300 Btu/hr with a cooling rate of 38,800 Btu/hr for a seasonal cooling COP of 0.57. The electrical accessory power for the water circulating pumps and air handler fan was 1.91 kw.

Monitored steady state performance at 1200 rpm showed a heating COP of 1.42 with a cooling COP of 0.60. Cycling effects during heating were shown to have a positive effect on heating efficiency because (1) a six minute spin down cycle was used after engine shut down and (2) the water-cooled condenser was in the same water loop with the engine jacket and exhaust heat exchanger. Cycling then led to a lower average condenser temperature and pressure while still recovering the engine heat through spin down.

The engine was found to be oversized for the compressor, resulting in only a 25% loading of the engine and a low engine efficiency of about 16¢. Variable engine speed tests from 1200 rpm to 1600 rpm showed a heating output increase of 20% with a drop in heating COP of 11%. The sensitivity of the heating efficiency to speed for this condenser-to-water-to-air system is expected to be greater than a direct condenser-to-air system.

The performance of the engine/compressor itself was measured for varying evaporator and condenser temperatures. These tests showed that for a 1^{o}F increase in condenser temperature, gas consumption increased 0.21%, condenser output decreased 0.49%, recovered engine/exhaust heat remained about constant, and the evaporator cooling rate decreased 0.81% with a 0.70% decrease in heating COP and 0.92% decrease in cooling COP. For a 1^{o}F increase in evaporator temperature, the gas consumption increased 0.48%, condenser output increased 2.56%, engine/exhaust heat recovery increased 0.39%, and the evaporator cooling rate increased 2.6% with the heating COP increasing 1.1% and the cooling COP increasing 2.1%.

Maintenance, Reliability and Noise

A major conclusion of this study concerns maintenance, reliability, and noise. During the 2400 operating hours over a 20 month period, no maintenance was performed. Oil analyses have been carried out and found to be completely within serviceable specifications. The specially tipped spark plugs have been checked and found to be within reasonable gap tolerance at 0.042 inch. Reliability has been 100% except for starting failures. Failure to start within the fixed five second starter engagement period would usually occur after a long period of not running. Manually resetting the controls was, the only action required to resume normal operation.

Noise levels in the equipment room were 63 dB with a 60 dB measured six feet from the outside exhaust.

In summary, the generally perceived problems of reliability, maintenance, and noise produced by and I.C. engine operating in the home have been shown not to be significant problems.

Analytical Air-to-Air Performance

A model was developed for calculating the performance of the same gas heat pump engine/compressor, but with air evaporator and air condenser coils in place of the water coils. Actual experimental data from the engine/compressor was used in the model. This data was then coupled with weather data in Chicago, Orlando, and Atlanta to yield annual performance efficiencies. The relative sizes of the indoor versus outdoor coils were optimized and performance was calculated for varying total coil size. For a fixed total investment in air coils, it was found that the indoor coil size should be about 60% of the outdoor coil size. Also, increasing the combined coil UA up to about 10,000 Btu/hr-^{o}F was found to be beneficial. Beyond this value minimal gas was conserved. For size scaling, this would mean a ratio of combined heat pump air coil UA per house UA of about 15, assuming the engine/compressor size was also scaled. This figure is not out of line with coil sizes used in present day electric heat pumps. At this value the seasonal heating COP's were 1.33, 1.45, and 1.53 for Chicago, Atlanta, and Orlando, respectively. All three cities showed a 0.73 seasonal cooling COP.

Recommendations

The water-to-water I.C. engine heat pump tested has shown reasonable efficiency and excellent short term (one to two years) maintenance and reliability. Advanced information also was obtained. The next potential problem areas for study should include long term engine durability, manufacturing and installation costs, air-to-air system performance, and defrost control.

The automotive derivative natural gas industrial engine tested has shown that this class of engine has merit. Continued study of the many available engines is needed to determine their suitability in terms of size, cost, and longevity.

Specifically, engines that are found to be suitably sized and available for this test application should undergo necessary modifications for gasification, such as cam shaft and compression ratio changes. Then two or three engines of each type should be run continuously at constant speed, and two or three should be run on a thirty minute start/stop basis. Long term engine life information can then be gained within about two years.

Simultaneously, an air-to-air heat pump with a matched engine/compressor should be field tested to study efficiencies and to optimize defrost strategy.